Journal of chemical & engineering data

Article

pubs.acs.org/jced

Multiphase Equilibria Modeling with GCA-EoS. Part II: Carbon Dioxide with the Homologous Series of Alcohols

Mariana González Prieto,[†] Francisco Adrián Sánchez,[†] and Selva Pereda*[,†,‡]

[†]Planta Piloto de Ingeniería Química (PLAPIQUI), Chemical Engineering Department, Universidad Nacional del Sur (UNS)—CONICET, Camino La Carrindanga Km7, 8000B Bahía Blanca, Argentina

[‡]Thermodynamics Research Unit, School of Engineering, University of KwaZulu-Natal, Howard College Campus, King George V Avenue, Durban 4041, South Africa

ABSTRACT: Modeling multiphase equilibria of mixtures comprising carbon dioxide (CO_2) and organic compounds is a challenge for any equation of state. CO_2 shows a highly nonideal phase behavior with most organic compounds, which is even more pronounced with hydrogen-bonding compounds. In this work, we have extended the Group-Contribution with Association equation of state (GCA−EOS) to represent vapor−liquid, liquid−liquid, and vapor−liquid−liquid equilibria of CO_2 mixtures with primary alcohols. The final set of parameters has been challenged against an experimental database covering C_1−C_{16} primary alcohols, temperatures from 230 to 573 K, and pressures up to 400 bar. Particular attention has been given to describe the critical curves for each binary system correctly, which means attaining the phase equilibria transformation of the CO_2 + 1-alcohol homologous series as the alcohol alkyl chain length increases. This parametrization strategy allows reducing the risk of incorrect liquid−liquid split predictions. In addition, using a single set of parameters, fitted to binary data of CO_2 with normal alcohols, the model is able to predict the phase behavior of binary mixtures not included in the parametrization procedure, comprising normal and branched alcohols. The GCA-EOS predicts properly the overall phase behavior, that is, the binary critical curves, without losing accuracy in the prediction of saturation points.

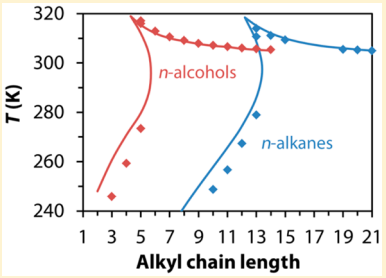

1. INTRODUCTION

Modeling overall multiphase equilibria of binary mixtures comprising carbon dioxide (CO_2) with homologous series of organic compounds (*n*-alkanes, *n*-alcohols, *n*-carboxylic acids, etc.) is a challenge for any equation of state. The task is more complex for a group contribution method, which uses a single set of interaction parameters for all the binaries of each homologous series. Even more so if we consider that the quadrupole moment of CO_2 highly affects the nonideality and phase behavior of these mixtures, causing multiple transformations between types of phase behavior, as the alkyl chain of the substrate increases. In Part I of this work,[1] we showed that GCA-EOS is able to describe the overall phase behavior of CO_2 + *n*-alkane mixtures using a single set of parameters under a wide range of conditions. Particularly, these mixtures undergo the following phase behavior transformation: Type II with alkanes up to *n*-undecane → Type IV with *n*-tridecane → Type III with higher alkanes,[2] according to the van Konynenburg and Scott[3] classification. The reader can find a detailed description of each type of behavior and their respective diagrams in Part I of this work.[1]

Peters et al. have long ago experimentally showed that self-associating substrates shift each transition to lower molecular weight substrates.[4−9] In addition, the stronger is the association, the greater is the displacement. For instance, in the case of the CO_2 + *n*-alcohol, homologues series under study in this work, the transformations occur as follows: Type II with alcohols up to *n*-butanol → Type IV with *n*-pentanol → Type III with higher *n*-alcohols.[2] Raeissi et al.[10] discussed in detail these transformations based on experimental evidence.

The prediction of phase behavior of mixtures comprising CO_2 and alcohols is important for multiple industrial applications. Because of its favorable physicochemical properties, CO_2 is the solvent par excellence in pressure-intensified technologies, also known as supercritical technologies. Particularly, CO_2 stands out for having near-room critical temperature, and being nonflammable, nontoxic, inert, and inexpensive.[11] In these technologies, alcohols are often used as cosolvents in order to improve the solubility of polar compounds in CO_2.[12,13] Another field of interest, and of high awareness today in the industrial and academic field, is that related to CO_2 capture and hydrate engineering.[14,15] The conceptual design of new technologies calls for thermodynamic models able of predicting CO_2 behavior with not only alcohols but also hydrocarbon and other potential solvents typically present in the gas and oil field. Also important, the oleochemical industry requires models for fatty alcohols, the thermodynamic modeling of which is substantially less studied in the literature.[16]

A literature review shows that many authors worked hard on the extension of advanced equations of state to model mixtures of

Special Issue: In Honor of Cor Peters

Received: July 18, 2017
Accepted: August 30, 2017

DOI: 10.1021/acs.jced.7b00663
J. Chem. Eng. Data XXXX, XXX, XXX−XXX

CO_2 with *n*-alcohols.[17−23] However, most of the studies only assessed a few alcohols, of either low[18,19,24] or high[25,26] molecular weight, and isolated projections of the overall phase behavior. As we showed in Part I of this work, fitting isothermal or isobaric equilibrium data, neglecting the binary critical curves and lower and upper critical points may lead to wrong predictions outside the correlated window. Furthermore, in systems showing partial liquid miscibility or multiphase behavior, that approach can trigger erroneous predictions of the types of phases in equilibrium, besides the wrong saturation points.[19,20]

Aware of the consequences of fitting only isothermal or isobaric behavior, some authors considered the overall phase behavior throughout the parametrization of different models. For instance, Polishuk et al.[27] proposed the Global Phase Diagram Approach (GPDA) to predict phase equilibria of homologues series. They modeled CO_2 + *n*-alcohols binary systems with C4-EOS. By adjusting key points of each binary system, they qualitatively predicted mixtures comprising alcohols from ethanol to 1-hexanol. On the other hand, Llovell and Vega[28] used the Soft−SAFT equation with a cross-over approach and included a quadrupolar term for CO_2. The authors correlated the binary system CO_2 + 1-pentanol, which is the only one showing the Type IV phase behavior. Using the same interaction parameters, they correctly predicted the type of phase behavior for 1-propanol and 1-butanol (Type II) and that of 1-hexanol (Type III). To our knowledge, no other author considered critical loci in the thermodynamic modeling of CO_2 + *n*-alcohols mixtures.

Another important aspect to take into account is the solvation between CO_2 and the alcohols. Many approaches have been used to describe the nonideality established by the quadrupole moment of the CO_2 and the dipole of the alcohols in advanced equations of state. For example, Gregg et al.,[29] using the HR-SAFT,[30] and Nguyen-Huynh et al.[31] using the GC-PPC-SAFT,[32] considered that CO_2 solvates with alcohols through one and two association sites, respectively. Gregg et al. estimated the cross-association parameters from spectroscopic data of CO_2 + 1-dodecanol,[33] while Nguyen-Huynh et al. applied the cross−association parameters of GC-PPC-SAFT available for H_2S with polar compounds to describe the phase equilibria of CO_2 + ethanol. By doing so, they attained good accuracy in that mixture, without fitting any extra binary interaction parameters. In particular, Oliveira et al.[17] and Tsivintzelis et al.[18] assessed the performance of the CPA-EOS. The latter compared the CPA accuracy when modeling CO_2 as a nonassociating, solvating, and even as self-associating specie. Tsivintzelis et al. also assessed the effect of assuming a different number of association sites in CO_2 (1 to 4). More recently, Bjørner and Kontogeorgis[34] evaluated the ability of qCPA-EoS to predict the phase equilibria of CO_2 with low molecular weight alcohols (methanol, ethanol, and propanol). qCPA is a new version of CPA that includes a quadrupolar contribution to the Helmholtz energy, in order to better describe the CO_2 interactions. They fitted a single interaction parameter per binary system to predict low to medium pressure phase equilibrium data at temperatures up to 350 K. The authors concluded that qCPA attains similar results to its previous version, that is, CPA considering solvation between CO_2 and alcohols, with fewer adjustable parameters.

This work is the second part of GCA-EOS extension to the multiphase behavior of mixtures comprising CO_2 and homologous series of organic compounds. Experimental data on the overall phase behavior of binary systems provides key information to train semiempirical thermodynamic models. It is important to highlight at this point that the group contribution approach allows predicting numerous compounds not included in the fitting procedure, based on the correlation of equilibrium information on good quality, such as the great deal of data sets reported by the laboratory of Prof. C.J. Peters. In Part I,[1] we thoroughly revised the binary interaction parameters between the paraffin and CO_2 groups, in order to accurately predict the phase behavior transformation of CO_2 + hydrocarbon mixtures, as the alkyl chain length increases. This work established a robust basis for further extending GCA-EOS to other organic families. In this follow up, we challenge the previous parametrization with the aim of modeling CO_2 + *n*-alcohols, using the same parametrization strategy. The experimental database includes C_1−C_{16} primary alcohols, temperatures from 230 to 573 K, and pressures up to 400 bar. Most of the data is left out of the optimization, in order to have experimental information to challenge the predictive capacity of the new set of parameters. In summary, the main focus of this study is to describe the transformation of phase behavior type, at the correct alkyl chain length, without losing accuracy in the prediction of saturation points.

2. THERMODYNAMIC MODELING

As we introduced before, the phase behavior of binary mixtures of CO_2 + *n*-alcohol homologues series undergoes the following transformation, as the alcohol alkyl chain increases: Type II with alkanes up to *n*-butanol → Type IV with *n*-pentanol → Type III with higher alcohols. This transformation must be described with a single set of binary interaction parameters when using group contribution models, by only changing the number of paraffin groups in the alcohol molecule. Therefore, in this work, the only interaction parameters to be fitted are those between the CO_2 and CH_2OH groups, since the interaction parameters between CO_2 and CH_3/CH_2 groups were already set to describe binary mixtures with hydrocarbons. This represents a particular challenge because the longer is the alkyl chain, the lesser is the influence of the new parameters. Thus, the parametrization should be done with low molecular weight alcohols. However, the new set has to correctly modify the phase behavior of high molecular weight alcohols, with respect to their homomorphous hydrocarbons, by only adding an alcohol group to the molecule.

The GCA-EOS model has three contributions to the residual Helmholtz energy. The two classic free volume and attractive contributions, represented by the extended Carnahan−Starling,[35] and a van der Waals term, respectively. The latter is combined with a density-dependent local-composition mixing rule, based on a group contribution version of the NRTL model.[36] Finally, the third contribution takes into account specific association interactions, using a group contribution version of the SAFT equation.[37] The reader can find details of the model equations in the Appendix.

Regarding the solvation between CO_2 and alcohols, several authors experimentally studied this interaction. Remarkable examples are the works of Hemmaplardh and King,[38] Coan and King,[39] and Gupta et al.,[40] who measured the second virial coefficient of highly diluted self-associating compounds (water, methanol, and ethanol) in different nonpolar supercritical solvents. They showed that the second virial coefficients were lower in CO_2 than in the other solvents, which suggests the existence of solvation interactions even in the gas phase. On the other hand, Fulton et al.[33] measured the nonassociated fraction of alcohols, from methanol to 1-dodecanol, in supercritical ethane and CO_2 using FT-IR spectroscopy. They found that the fraction of the alcohol self-associated molecules is smaller in

DOI: 10.1021/acs.jced.7b00663
J. Chem. Eng. Data XXXX, XXX, XXX−XXX

Table 1. Pure *n*-Alcohol Critical Temperatures and Diameters for the Model Free-Volume Contribution. GCA-EoS Accuracy To Predict Critical Points and Vapor Pressure in the Reduce Temperature Range (ΔT_r). Experimental data from DIPPR[51]

cmpd	T_c (K)	d_c[a] (cm mol$^{-1/3}$)	ARD% (T_c)[b]	ARD% (P_c)[b]	ΔT_r	AARD (P^v)%[c]
methanol	512.6	3.1531	0.3	1.6	0.50−0.95	1.4
ethanol	514.0	3.5876	0.0	0.1	0.52−0.95	0.7
1-propanol	536.8	4.0297	0.4	0.7	0.53−0.95	1.7
1-butanol	563.0	4.4000	0.5	1.0	0.60−0.95	1.7
1-pentanol	588.1	4.7390	1.1	0.4	0.53−0.95	2.5
1-hexanol	610.3	5.0341	0.9	0.3	0.53−0.95	2.7
1-heptanol	632.6	5.3109	1.0	0.4	0.54−0.95	4.3
1-octanol	652.5	5.5775	0.7	0.7	0.55−0.95	4.5
1-nonanol	670.7	5.8240	1.3	1.6	0.55−0.95	4.2
1-decanol	687.3	6.0616	1.3	1.5	0.55−0.95	4.2
1-undecanol	703.6	6.2967	1.7	3.4	0.56−0.95	3.4
1-dodecanol	719.4	6.4984	1.6	2.9	0.57−0.95	4.8
1-tridecanol	734.0	6.7026	1.6	6.6	0.57−0.95	4.6
1-tetradecanol	744.9	6.9043	1.4	5.2	0.58−0.95	4.6
1-pentadecanol	759.0	7.0923	1.6	7.8	0.58−0.95	4.4
1-hexadecanol	770.0	7.2828	1.2	5.0	0.59−0.95	4.2
1,2-ethanediol	720.0	3.7510	3.5	8.2	0.50−0.79	10
1,8-octanediol[d]	752.0	5.6085	1.6	11	–	–

[a]Critical diameter fitted to a pure compound saturation point, except for molecularly modeled compounds (methanol and ethanol), the critical diameters of which are calculated to fulfill the critical constraints.[50] [b]ARD: Absolute relative deviation in critical temperature and pressure. [c]AARD: Average absolute relative deviation in vapor pressure in the temperature range ΔT_r [d]1,8-Octanediol experimental critical properties are from Nikitin et al.[52]

Table 2. Pure Group Parameters of the Attractive Contribution of GCA-EOS

group i	q_i	T_i* (K)	g_i* (atm cm^6 mol^{-2})	g_i'	g_i''	ref
CH_3	0.848	600	316910	−0.9274	0	53
CH_2	0.540	600	356080	−0.8755	0	53
CO_2	1.261	304.20	531890	−0.5780	0	53
CH_3OH	1.432	512.60	547425	−0.6195	0.2488	50
C_2H_5OH	1.972	514.00	438929	−0.6945	0.1448	50
CH_2OH	1.124	512.60	531330	−0.3201	−0.0168	50

Table 3. Binary Energy Interaction Parameters Between Attractive Groups

group						
i	j	k_{ij}*	k_{ij}'	α_{ij}	α_{ji}	ref
CO_2	CH_3OH	0.9146	−0.0788	2.0	0	this work
	C_2H_5OH	0.9268	0.0408	−9.1	0	this work
	CH_2OH	0.9084	0.080	−5.0	0	this work
CH_2OH	CH_3	0.895	−0.090	0	0	50
	CH_2	1.020	0.005	0	0	50

Table 4. Self and Cross-Associating Parameters of GCA-EOS

site k	group i	site l	group j	$\varepsilon_{ki,lj}R^{-1}$/K	$\kappa_{ki,lj}$ / (cm^3 mol^{-1})	ref
(+)	OH	(−)	OH	2759	0.8709	50
(+)	CO_2	(−)	OH	1583	1.5214	this work

CO_2 than in ethane, telling again the existence of a weak CO_2−alcohol complex. Furthermore, several authors[41−43] have studied this association interaction using ab initio methods. Specifically, they reported evidence of electron donor−acceptor (EDA) interaction between the carbon atom of the CO_2 and the electrons of the oxygen of the polar compound. However, Saharay et al.[43] also reported evidence of hydrogen bond formation between ethanol and CO_2; although, they showed that EDA interactions are favored over hydrogen bonding. Moreover, Monte Carlo studies of ethanol in supercritical CO_2 also showed evidence that hydrogen bond formation is less favored than EDA.[44]

On the basis of these observations, we treated CO_2 as an electron acceptor specie. Moreover, before setting the number of associating sites of CO_2 (M_{CO2}), we evaluated the dependence upon this parameter of the GCA-EOS association contribution to the fugacity coefficient, at both infinite dilution extremes. Soria et al.[45] gave the expression for the GCA-EoS association contribution to the fugacity coefficient of a component j in the mixture, $\hat{\varphi}_j^{assoc}$:

$$\ln \hat{\varphi}_j^{assoc} = \sum_{i=1}^{NGA} \nu_i^* \sum_{k=1}^{M_i} \ln X_{ki} \tag{1}$$

where the fraction of groups i nonbonded through site k (X_{ki}) is set by the expression:

$$X_{ki} = \left(1 + \sum_{j=1}^{NGA} \sum_{l=1}^{M_j} \frac{n_j^* X_{lj} \Delta_{ki,lj}}{V}\right)^{-1} \tag{2}$$

the summation includes all associating groups (NGA) with M_j sites. Finally, X_{ki} also depends on the strength of association, $\Delta_{ki,lj}$:

$$\Delta_{ki,lj} = \kappa_{ki,lj}\left[\exp\left(\frac{\varepsilon_{ki,lj}}{RT}\right) - 1\right] \tag{3}$$

It is worth noting that the radial distribution function was set to a constant value of one in the GCA-EOS, in order to attain a group

DOI: 10.1021/acs.jced.7b00663
J. Chem. Eng. Data XXXX, XXX, XXX−XXX

Table 5. GCA-EoS Phase Behavior Correlation of CO_2 + *n*-Alcohols Binary Systems

vapor−liquid equilibria						
			AARD%[a]			
alcohol	T/K	P/bar	P	y_1	no. expt points	ref
methanol	230, 373	7.0−120	7.0	2.4	15	55, 56
	373	20−54	7.6		12	57
	373	20−54		4.4	13	57
ethanol	293, 353	7.0−120	3.8	1.3	13	58, 59
1-butanol	293, 430	6.3−145	5.2	1.0	15	46, 47
1-hexanol	293	8.0−55	8.2	0.23	7	48
1-heptanol	293	7.0−57	5.3	0.40	9	49
liquid−liquid equilibria						
			AAD[a] (AARD%) of x_i in j			
alcohol	T/K	P/bar	CO_2 in alcohol	alcohol in CO_2	no. expt points	ref
1-hexanol	293	55−68	0.024 (3.1)	0.034 (51)	6	48
1-heptanol	293	57−124	0.020 (2.8)	0.037 (81)	19	49

[a]AAD and AARD%: average absolute and relative deviations in pressure (P) and composition (x/y), respectively.

contribution version of SAFT, which allows describing all alcohols with a single set of association parameters (ε and κ).

From eq 1 and 2, the association contribution to the fugacity coefficient of alcohols at infinite dilution ($\hat{\varphi}^{\text{assoc},\infty}_{\text{Alcohol}}$) is

$$\ln \hat{\varphi}^{\text{assoc},\infty}_{\text{Alcohol}} = \ln X^{\infty}_{\text{OH}(-)} = \ln\left(\frac{1}{1 + M_{\text{CO2}}\Delta_{\text{cross}}\rho_1}\right) \tag{4}$$

where $X^{\infty}_{\text{OH}(-)}$ is the nonbonded fraction of the electronegative site of the OH association group at infinite dilution. It is important to note that, in the infinite dilution limit, the contribution of the positive site of the OH group vanishes because the alcohol group is surrounded only by CO_2, which does not have electronegative sites. M_{CO2} is the number of association sites of the CO_2 group, Δ_{cross} is the cross−association force between the negative site of the OH group and the positive site of CO_2, and ρ_1 is the density of pure CO_2. Note that, if eq 3 is replaced in eq 4, as long as the product $M_{\text{CO2}} \times \kappa_{\text{cross}}$ remains constant, the association contribution to the alcohol fugacity coefficient will not change for different values of M_{CO2}.

On the other hand, the association contribution to the fugacity coefficient of CO_2 in alcohol, also at infinite dilution ($\hat{\varphi}^{\text{assoc},\infty}_{\text{CO2}}$), is

$$\ln \hat{\varphi}^{\text{assoc},\infty}_{\text{CO2}} = M_{\text{CO2}} \ln X^{\infty}_{\text{CO2}(+)} = M_{\text{CO2}} \ln\left(\frac{1}{1 + X^{\text{pure}}_{\text{OH}(-)}\Delta_{\text{cross}}\rho_2}\right) \tag{5}$$

where $X^{\infty}_{\text{CO2}(+)}$ is the nonbonded fraction of the electropositive sites of CO_2 at infinite dilution, ρ_2 is the density of pure alcohol, and $X^{\text{pure}}_{\text{OH}(-)}$ is the nonbonded fraction of the electronegative site of the OH association group in pure alcohol. Thus, in this case, the association contribution to the fugacity coefficient *is* proportional to the number M_{CO2}. Nonetheless, its effect is negligible, since $X^{\infty}_{\text{CO2}(+)}$ is close to 1. In other words, strong hydrogen-bonding compounds such as alcohols are highly self-associated in the pure limit; therefore, $X^{\text{pure}}_{\text{OH}(-)}$ is close to zero (see right-hand side of eq 5. In this case, the effect of M_{CO2} is small, if any, and easy to correct through small perturbations in the interaction parameters.

In conclusion, the effect of using different values of M_{CO2} can be compensated with a proper value of volume of cross-association (κ_{cross}) in binary mixtures that exhibit a weak cross association.

In accordance with this analysis, Tsivintzelis et al.[18] show that a CO_2 + alcohol binary mixture can be fitted indistinctly with the CPA-EOS, assuming one or two association sites in the CO_2 molecule. In consequence, we modeled CO_2 as a solvating specie, able to cross-associate as an electron acceptor. Furthermore, we arbitrarily set as two the number of associating sites of the CO_2 molecule, since a value of one leads to an unusually high value of the OH/CO_2 cross association volume.

The parametrization procedure was performed through the optimization of the following objective function:

$$\text{OF} = \sum_{i=1}^{N_{\text{eq}}} {e_{\text{eq},i}}^2 \tag{6}$$

where N_{eq} is the number of equilibrium points and $e_{\text{eq},i}$ is the error between experimental and calculated data as follows:

$$e^2_{\text{eq},i} = \text{IFL}_i {w_{p_i}}^2 (P_{\text{exp},i} - P_{\text{calc},i})^2 + (1 - \text{IFL}_i) {w_{x_i}}^2 (x_{\text{exp},i} - x_{\text{calc},i})^2 + {w_{y_i}}^2 (y_{\text{exp},i} - y_{\text{calc},i})^2 \tag{7}$$

where P is the pressure, x and y the molar fraction in the liquid and vapor phase, w_P, w_x, and w_y are the weighting factors in P, x, and y, and IFL is an auxiliary variable which sets the type of flash calculations: 0 for a *TP* flash and 1 for bubble point calculations.

In this work, all binary VLE systems were evaluated through bubble point calculation, while a *TP* flash was used for LLE and supercritical fluid−liquid equilibrium (SFLE) data. Likewise in Part I of this work, the weighting factor of each experimental data point was set equal to the inverse of its value. Even though we did not fit critical curves, in order to improve the predictions of the critical loci, we gave more weight to equilibrium data nearby the critical points. Particularly, we increased the weighting factor of the two data points closest to the critical behavior by a factor of 10. The objective function (eq 6) was minimized drawing upon the Levenberg−Marquardt algorithm of finite difference coded in Fortran77.

In addition, we built and assessed an extensive phase equilibria database, including 30 binary systems of CO_2 with primary alcohols, both linear and branched alkyl chains with up to 16 carbon atoms. The part of the database used for correlation only includes binary systems with 1-butanol, 1-hexanol and 1-heptanol at several temperatures,[46−49] to fit the residual interaction and

DOI: 10.1021/acs.jced.7b00663
J. Chem. Eng. Data XXXX, XXX, XXX−XXX

Table 6. GCA-EoS Phase Behavior Prediction of CO_2 + *n*-Alcohols Binary Systems

alcohol	T/K	P/bar	AARD%[a] P	AARD%[a] y_1	no. expt points	ref
vapor−liquid equilibria						
methanol	230−477	4.0−65	5.1	3.9	354	57, 58, 60−69
	243−473	2.0−161	4.6		80	57, 70, 71
	242−473	4.0−161		3.3	43	57
ethanol	238−453	5.0−150	5.2	0.8	286	58−60, 62, 63, 68, 72−79
	291−373	17−141	9.9		60	80, 81
1-propanol	293−427	5.0−159	6.7	1.2	142	47, 63, 71, 82−84
1-butanol	303−427	5.2−170	5.1	0.6	169	46, 47, 74, 85−89
1-pentanol	293−317	5.0−84	5.5	0.4	48	88, 90−92
	303, 313	53−83	4.3		10	93
1-hexanol	303	7.0−69	3.0	0.5	10	48
	303	7.7−66	4.6		10	94
1-heptanol	292, 298, 303	6.0−71	6.0	0.4	23	49, 95, 96
1-octanol	308	15−77	9.3	0.16	12	67
1-nonanol	303	13−71	7.5	0.13	8	97

alcohol	T/K	P/bar	AAD[a] (AARD%) of x_i in j: CO_2 in alcohol	AAD[a] (AARD%) of x_i in j: alcohol in CO_2	no. expt points	ref
liquid−liquid equilibria						
1-hexanol	303	69−79	0.022 (2.8)	0.030 (50)	4	48
	303	71−80	0.058 (7.9)		5	94
1-heptanol	292, 298, 303	59−108	0.045 (6.0)	0.035 (612)	22	49, 95, 96
1-octanol	298, 303	52−128	0.11 (19)	0.038 (307)	8	96
	308	68−117.1	0.074 (12)		3	98
	308	80−126		0.016 (77)	5	98
1-nonanol	303	71−150	0.073 (11)	0.022 (142)	6	73, 97
supercritical fluid−liquid equilibria						
1,2-ethanediol	298−398	0.29−203	0.016 (27)		39	99
	273−423	30, 58		2.5×10^{-4}(16)	14	99
1-pentanol	323−427	6−187	0.039 (8.6)	0.018 (44)	105	88, 90−92, 100, 101
	323−373	72−170	0.058 (9.1)		18	93
1-hexanol	313−432	6.0−202	0.051 (9.5)	0.016 (42)	85	48, 102
1-heptanol	313−432	11−212	0.047 (10)	0.018 (89)	78	49, 95, 96, 102
1-octanol	313−453	10−213	0.034 (8.4)	0.003 (37)	93	67, 96, 103−106
	313−348	33-212	0.037 (6.3)		45	98, 107
	313−348	94−182		0.015 (32)	35	98, 107
1-nonanol	308−353	12−156	0.031 (8.0)	2×10^{-3} (67)	60	67, 97
1,8-octanediol	393	100−400	0.022 (7.1)	1.2×10^{-3} (38)	7	108
1-decanol	308−453	10−190	0.040 (12)	3×10^{-3} (37)	70	67, 103, 104
	308.5−348.5	76−205	0.040 (5.97)		24	26
1-undecanol	353, 373, 393	100−260	0.056 (9.1)	0.011 (26)	18	109
1-dodecanol	333, 353, 393	99−275	0.047 (7.0)	9×10^{-3} (48)	17	110−112
1-tridecanol	323	84−240		0.015 (100)	14	112
1-tetradecanol	373, 423, 473	10−51	0.014 (9.7)	5×10^{-3} (79)	15	113
1-pentadecanol	323	90−237		0.012 (137)	14	112
1-hexadecanol	373−573	10−323	0.020 (8.3)	5×10^{-3} (67)	25	111, 113
1-octadecanol	373, 473, 573	10−50.7	0.015(9.7)	0.002 (63)	15	113
vapor−liquid−liquid equilibria						
1-hexanol	255−309	28−79	0.025 (4.2)	9.0×10^{-3} (23)	10	114
1-heptanol	289−310	51−81	0.035 (5.2)	9.0×10^{-3} (33)	22	49
1-octanol	250−306	18−75	0.034 (6.1)	0.011 (79)	12	115
1-decanol	270−307	32−78	0.058 (10)	7.9×10^{-3} (82)	11	114

[a]AAD and AARD%: average absolute and relative deviations in pressure (P) and composition (x/y), respectively.

solvation parameters of CH_2OH/CO_2. Moreover, the first compounds of the homologous series (methanol and ethanol) were modeled molecularly, which means that also part of their binary data was correlated. More details on the parametrization procedure can be found in Part I of this work.[1]

3. RESULTS AND DISCUSSIONS

3.1. Modeling CO_2 + *n*-Alcohol Mixtures. As already introduced, to develop a robust group contribution model to predict multiphase behavior, it is essential to challenge the model to follow up the transformation between types of phase behavior

DOI: 10.1021/acs.jced.7b00663
J. Chem. Eng. Data XXXX, XXX, XXX−XXX

as the alkyl chain length increases. It is important to keep in mind that the current parametrization is based on previous works modeling pure alcohols.[50] Group contribution models must describe the vapor pressure of the whole *n*-alcohol homologous family with three groups (CH_2, CH_3, and CH_2OH). Moreover, binary interaction between *n*-alcohols and the CO_2 group should be based in previous parametrization of the phase behavior of CO_2 with hydrocarbons,[1] which set parameters for CO_2/CH_2−CH_3 interaction.

Table 1 lists for all the *n*-alcohols under study the critical temperature and diameter (parameters of the model free-volume contribution) and the accuracy of the GCA-EOS to predict their critical points and vapor pressure, in the indicated reduced temperature range. As can be observed, the GCA-EOS predicts accurately the critical points and vapor pressures of all the *n*-alcohols under study in this work.

On the other hand, Table 2 shows pure surface energy parameters for the attractive term of all groups involved in CO_2 + *n*-alcohol binary systems, together with the source of these parameters. It is important to highlight that all the groups used in this work were defined in previous contributions and none of them required refitting. Moreover, Table 3 reports the binary interaction parameters for the attractive term. Last, Table 4 shows the self-association parameters of the hydroxyl group, determined by Soria et al.[50] and the weak cross-association between CO_2 and the hydroxyl group, regardless to which alcohol it belongs. The reader should notice that the only new parameters, to model the whole *n*-alcohol series with CO_2, are the six binary interactions between CO_2 and the alcohol group (four for the attractive term and two for the association term). In addition, methanol and ethanol, like any first compounds of a series, are modeled as molecular groups. Therefore, they have their own binary interaction parameters with CO_2, but still share with the rest of the alcohols the solvation parameters.

Regarding binary systems, Tables 5 and 6 show the GCA-EOS correlation and prediction of the binary systems CO_2 + *n*-alcohols, respectively. These tables also report the temperature and pressure range covered by the experimental data, number of data points, and source of the experimental data for each binary system. It is worth noting that the relative deviations of LLE and SFLE data are calculated relative to the minority compound in each phase. Furthermore, as we have already stated, we did not leave out any experimental data of the predicted database, even though there is disagreement between some sets of different authors, as shown in a previous literature review.[54]

The model predicts accurately the bubble pressure and vapor phase composition of VLE data of alcohols between methanol and 1-nonanol, with an average deviation of 5.4% and 1.6%, respectively. In the case of LLE and SFLE, the average absolute deviations are about 0.03−0.05 in mole fraction for both phases. Naturally, the relative error in the CO_2-phase is higher since the alcohol solubility in liquid CO_2 is, in general, below 2% in molar basis. On the other hand, Figure 1 shows the experimental upper and lower critical end points for the CO_2 + *n*-alcohol binary systems as the alkyl chain increases. These data allow inferring the type of phase behavior for each binary and, consequently, its transformation within the homologous family, namely, binary behavior changing from Type II (lower than C_5) to III (higher than C_5), going through Type IV at 1-pentanol. Figure 1 also depicts that GCA-EOS is able to follow up the phase transition of the homologous series under study. Furthermore, Figure 2 shows the model prediction of the critical loci of selected binary systems. Overall, a very good description is obtained for the whole series.

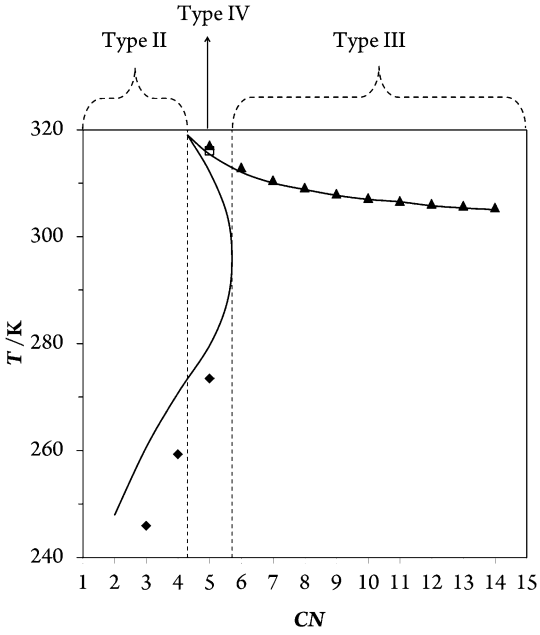

Figure 1. Transformation between types of fluid phase behavior of CO_2 + *n*-alcohol binary systems. Symbols: experimental data of UCEP (♦,▲) and LCEP (□).[10] Lines: GCA-EOS predictions.

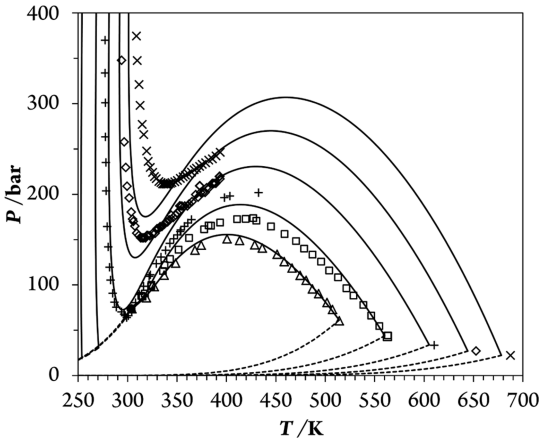

Figure 2. *PT* projection of the phase behavior of selected CO_2 + *n*-alcohols binary systems: (△) ethanol; (□) 1-butanol; (+) 1-hexanol; (◇) 1-octanol; and (×) 1-decanol. Symbols: experimental data.[51,62,75,88,96,102,104,115−118] Solid lines: GCA-EoS predictions of critical lines. Dashed lines: GCA-EoS prediction of pure compound vapor pressure curves.

It is worth noting that a good description of the *PT* projection of the whole *n*-alcohol family means that the model will perform well in multiphase behavior with a single set of parameters.

Figures 3 and 4 show isothermal phase equilibria progression of selected CO_2 + *n*-alcohol binary systems, covering alcohols of different alkyl chain lengths (C_1 to C_{16}) and temperatures from 293 to 393 K. To help visualization, Figure 3 reports composition in weight basis, while Figure 4 is in the usual molar basis. In general, GCA-EOS describes well the temperature dependence of the VLE behavior, as well as the effect of changing the alcohol alkyl chain length, using a single set of parameters. Moreover, the model predictions of alkanediols such as 1,8-octanediol follow qualitatively well the experimental data. Last, Figure 5 shows the experimental VLLE of different CO_2 + *n*-alkanol binary systems and the GCA-EOS predictions, which qualitatively describe the data.

DOI: 10.1021/acs.jced.7b00663
J. Chem. Eng. Data XXXX, XXX, XXX−XXX

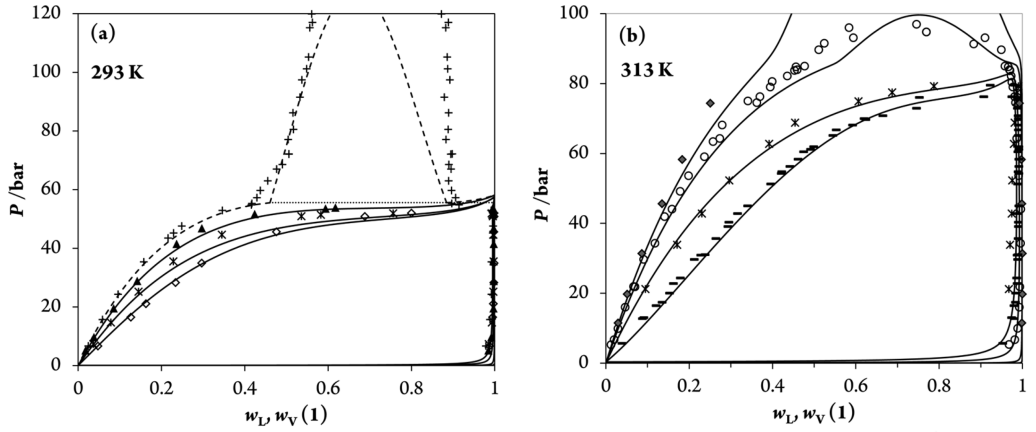

Figure 3. Vapor−liquid equilibria of CO_2 + *n*-alcohols with alkyl chain length between C_1 to C_9 (compositions in mass basis): (a) (◇) ethanol; (∗) 1-propanol; (▲) 1-pentanol; and (+) 1-heptanol at 293 K. (b) (−) methanol; (∗) 1-propanol; (○) 1-hexanol; and (×) 1-nonanol at 313 K. Symbols: experimental data.[48,55,65,67,82,94,97] Dashed and solid lines: GCA-EOS correlation and predictions, respectively. Dotted lines: predicted VLLE.

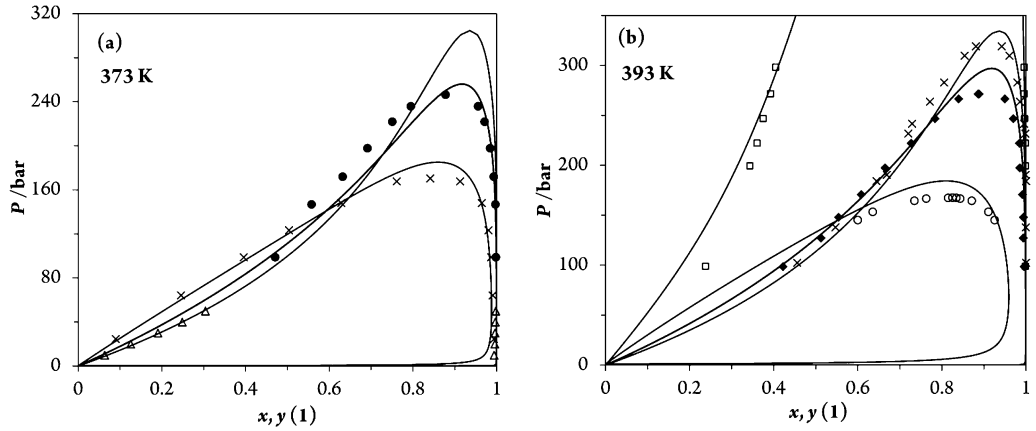

Figure 4. Vapor−liquid equilibria of CO_2 + *n*-alcohols with alkyl chain length between C_3 to C_{16} (compositions in molar basis): (a) (×) 1-propanol; (●) 1-undecanol; and (△) 1-hexadecanol at 373 K. Symbols: experimental data.[100,109,113] (b) (○) 1-butanol; (♦) 1-dodecanol; (×) 1-hexadecanol; and (□) 1,8-octanediol at 393 K. Symbols: experimental data.[88,108,111] Solid lines: GCA-EoS predictions.

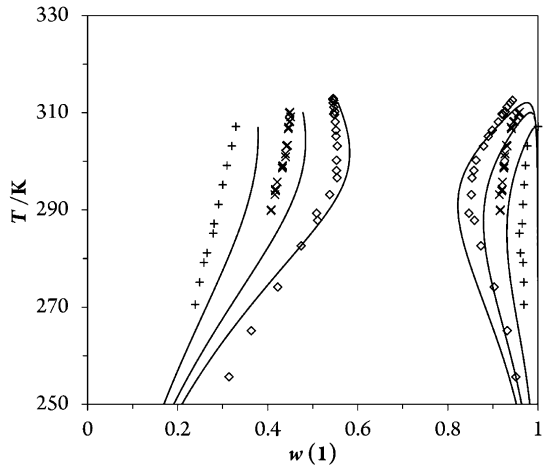

Figure 5. Vapor−liquid−liquid equilibria of the binary systems CO_2 (1) + *n*-alcohol: (◇) 1-hexanol; (×) 1-heptanol; and (+) 1-decanol (compositions in mass basis). Symbols are experimental data[48,95,114,115] and solid lines are the GCA-EOS predictions.

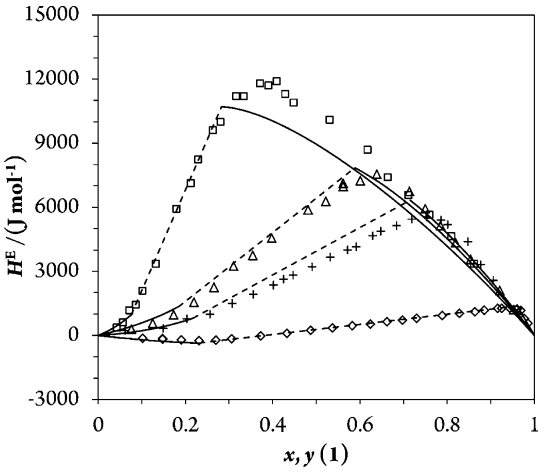

Figure 6. Excess enthalpy of CO_2 (1) + *n*-alcohols (2) at 473 K and 75 bar. Symbols: experimental data[119] of (□) methanol, (△) 1-propanol, (+) 1-butanol, and (◇) 1-octanol. Lines: GCA-EOS predictions. Dotted lines: predicted two-phase region.

Although excess properties were not included in the parametrization procedure, the model should predict them, at least qualitatively, since we fitted the set of parameters covering a wide range of temperature and pressure.[1] As an example, Figure 6 depicts the prediction of the excess enthalpy of CO_2 + different *n*-alcohols (methanol, 1-propanol, 1-butanol and 1-octanol) at constant temperature and pressure. The model predicts well the tendency in the excess enthalpy as the alkyl chain length increases.

DOI: 10.1021/acs.jced.7b00663
J. Chem. Eng. Data XXXX, XXX, XXX−XXX

Table 7. Pure Group Parameters of the Attractive Contribution of GCA-EOS

group i	q_i	T_i^* (K)	g_i^* (atm cm^6 mol^{-2})	g_i'	g_i''	ref
$CHCH_3/CHCH_2$	1.076/0.768	600	303749	−0.8760	0	45
$(B)CH_3$	0.848	600	282715	−0.6393	0	45
$(B)CH_2$	0.540	600	294523	−0.8233	0.07	45

Table 8. Binary Energy Interaction Parameters for Branched Alkyl Groups

group						
i	j	k_{ij}^*	k_{ij}'	α_{ij}	α_{ji}	ref
CO_2	$CH_3/(B)CH_3$	0.9185	0.0469	−26.0	4.0	1
	$CH_2/(B)CH_2/CHCH_3/CHCH_2$	0.9100	0.0469	−21.0	0	1
CH_2OH	$CHCH_3/CHCH_2$	0.9424	−0.10	0	0	45
	$(B)CH_3/(B)CH_2$	0.9680	−0.0424	0	0	45

3.2. Prediction of Phase Equilibria of Branched Alcohols. In the same way as with *n*-alcohols, we first evaluated the accuracy of the model to predict pure compound critical points and vapor pressure data of branched alcohols. To assemble a branch alcohol by group contributions, the branched alkyl groups are needed. Soria et al.[45] explained in detail the GCA-EOS parametrization of branched alkyl chains and how to assemble compounds. Moreover, in Part 1 of this work,[1] we also fitted the interaction between the groups of branched hydrocarbons and CO_2. Table 7 shows pure surface energy parameters for the attractive term of those groups, together with the source of the parameters. Moreover, Table 8 lists their binary interaction parameters. Again, the reader should notice that all these parameters were defined in previous contributions and none of them required refitting. Last, branched alcohols use the same association parameters reported for *n*-alcohols (see Table 4).

Table 9 lists the critical temperature and diameter of branched alcohols reviewed in this work, parameters of the model free-volume contribution, and the GCA-EOS accuracy to predict their critical points and vapor pressure when experimental data are available. Because the critical properties of some branched alcohols are not available in the open literature, we used the method developed by Scilipoti et al.[120] to estimate their critical temperature.

Table 10 reports GCA-EOS predictions of phase equilibria of CO_2 + branched alcohols binary systems. It should be mentioned that all cases are full prediction, based on the parameters of previous works and those for linear alcohols fitted in this work. Table 10 also gives the pressure and temperature range covered by the experimental data, the number of experimental data points, and their source. On the other hand, Figure 7 shows experimental and predicted critical locus of selected branched alcohols. The model follows qualitatively the critical experimental data. Regarding the VLE prediction, the GCA-EOS is able to fully predict the phase behavior of branched alcohols with an average relative deviation of about 10%. However, we found for branched alcohols several inconsistent experimental data sets of different authors. For instance, Sima et al.[128] reviewed deeply the binary system CO_2 + 2-methyl-1-propanol, comparing different sources of experimental data. Figure 8 shows the scattered isothermal VLE data available for CO_2 + 2-methyl-1-propanol. As can be seen, bubble pressure data measured at different temperatures by unlike authors superpose each other incorrectly. Another case that deserves discussion is that of pentanol isomers: Ionomata et al.[129] and Lin et al.[130,131] showed that, at a given temperature, mixtures of CO_2 and the isomers 2-methyl-1-butanol and 3-methyl-1-butanol have very similar bubble pressure, as well as GCA-EOS predicts for these two isomers. However, GCA-EOS is in better agreement with the data of Lopes et al.,[132] Gutierrez et al.,[82] and Vázquez da Silva et al.[133] (ARD(P) = 7.3% for 3-methyl-1-butanol) than that of Ionomata et al.[129] and Lee et al.[130,131] (ARD(P)= 17% and 10%, for 2-methyl-1-butanol and 3-methyl-1-butanol, respectively). On the other hand, GCA-EOS does not predict accurately the data of Hsieh et al.[20] for the CO_2 + 2,2-dimethyl-1-propanol binary system, ARD(P) = 18%).

Finally, Schwarz et al.[25] presented an interesting study about the effect of side branching of C_8-alcohols in supercritical CO_2. Up to our knowledge, there is no experimental information about the type of phase behavior depicted by these alcohols with CO_2. Nonetheless, Figure 9 shows that the GCA-EoS can predict the phase behavior of the structural isomers, as well as its temperature dependence.

3.3. Effect of the Number of Association Sites in the CO_2 Molecule. In the Thermodynamic Modeling section we show that the association fugacity coefficients of alcohol and

Table 9. Pure Branched Alcohol Critical Temperatures and Diameters for the Free-Volume Contribution of GCA-EOS. Model Accuracy To Predict Critical Points and Vapor Pressure in the Reduce Temperature Range (ΔT_r). Experimental data from DIPPR,[51] unless Another Source Is Indicated

cmpd	T_c (K)	d_c[a] (cm mol$^{-1/3}$)	ARD% (T_c)[b]	ARD% (P_c)[b]	ΔT_r	AARD (P^v)%[c]	ref
2-methyl-1-propanol	547.8	4.3977	1.4	2.8	0.60−0.95	2.4	51
2-methyl-1-butanol	575.4	4.7288	1.7	6.6	0.54−0.95	3.6	51
3-methyl-1-butanol	577.2	4.7057	1.2	3.9	0.54−0.95	2.5	51
2,2-dimethyl-1-propanol	550.0	4.7574	0.1	10	0.61−0.95	2.3	51
2-methyl-1-pentanol	604.4	5.0383	2.7	5.5	0.53−0.95	6.6	51
2,2,4-trimethyl-1-pentanol	629.9[d]	5.5909			0.53−0.70	9.5	121, 122
2,4,4-trimethyl-1-pentanol	629.9[d]	5.5068			0.56−0.71	5.8	121, 123
2-ethyl-1-hexanol	640.6	5.5715	2.2	5.7	0.60−0.95	7.6	51
2-propyl-1-pentanol	642.5[d]	5.6165					124
3,7-dimethyl-1-octanol	670.8[d]	6.0428			0.54−0.58	12	125−127

[a]Critical diameter fitted to a pure compound saturation point. [b]ARD: Absolute relative deviation in critical temperature and pressure. [c]AARD: Average absolute relative deviation in vapor pressure in the temperature range ΔT_r. [d]Calculated with the method proposed by Scilipoti et al.[120]

DOI: 10.1021/acs.jced.7b00663
J. Chem. Eng. Data XXXX, XXX, XXX−XXX

Table 10. GCA-EoS Phase Behavior Prediction of CO_2 + Branched Alcohols Binary Systems[a]

vapor−liquid equilibria						
			AARD%[a]			
alcohol	T/K	P/bar	P	y_1	no. expt points	ref
2-methyl-1-propanol	288−353	15−128	7.2[b1]	0.8	58	128, 133
	273−313	4.6−80	16[b1]		51	134, 135
	313−353	20−139	12[b1]	0.6	94	82, 129, 136, 137
2-methyl-1-butanol	313, 333	11−97	17[b2]	0.2	16	129, 130
3-methyl-1-butanol	313, 323	55−107	6.2[b2]		11	132
	313, 323	53−95	−	0.21	13	132
	288−333	12−105	7.5[b2]	1.3	83	82, 133
	313, 333	20−107	10[b2]	0.6	17	129, 131
2,2-dimethyl-1-propanol	333, 353	31−133	18		16	20
2-methyl-1-pentanol	348, 403, 453	7.0−197	12	1.0	32	103, 104
2,2,4-trimethyl-1-pentanol	308, 328, 348	52−144	4.3		21	25
	308, 328, 348	105−142		1.0	10	25
2,4,4-trimethyl-1-pentanol	308, 328, 348	53−156	4.7		22	25
	308, 328, 348	108−146		1.6	9	25
2-ethyl-1-hexanol	308, 328, 348	66−175	6.0		18	25
	308, 328, 348	75−159		1.3	48	25
2-propyl-1-pentanol	308, 328, 348	63−163	4.7		17	25
	308, 328, 348	76−157		1.1	21	25
3,7-dimethyl-1-octanol	307−349	71−198	5.8		43	26

[a]AARD%: average absolute and relative deviations in pressure (P), and composition (y), respectively. [b1]Experimental data from different authors are inconsistent (see text for extended discussion). [b2]Experimental data from different authors are inconsistent (see text for extended discussion).

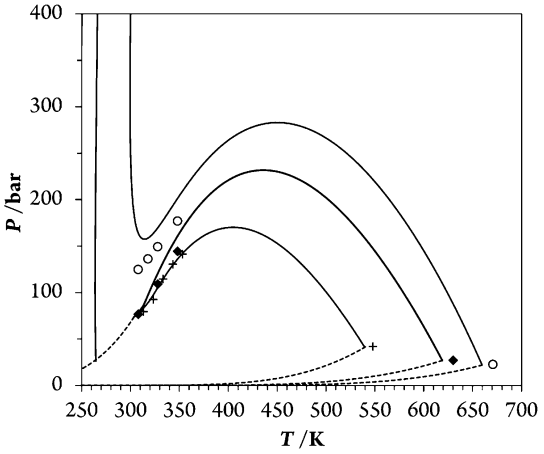

Figure 7. *PT* projection of the phase behavior of selected CO_2 + branched alcohols: (+) 2-methyl-1-propanol; (◆) 2,4,4-trimethyl-1-pentanol; and (○) 3,7-dimethyl-1-octanol. Symbols: experimental data.[25,26,51,120,137] Solid lines: GCA-EoS predictions of critical lines. Dashed lines: GCA-EoS prediction of pure compound vapor pressure curves.

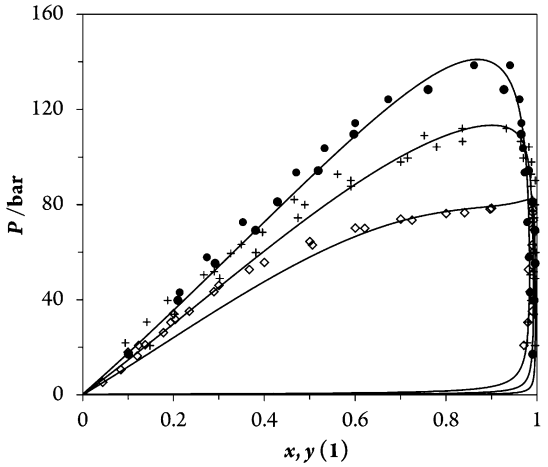

Figure 8. Phase equilibria of the system CO_2 (1) + 2-methyl-1-propanol (2) at (◇) 313.15 K, (+) 333 K, and (●) 353 K. Symbols represent experimental data;[82,128,134,135,137] solid lines are model predictions.

CO_2, at infinite dilution, do not depend on the number of association sites in the CO_2 molecule (M_{CO2}), but rather on the product $M_{CO2} \times \kappa_{cross}$. Therefore, we arbitrarily set the value of M_{CO2} in 2. After fitting the cross-association parameters between CO_2 and the hydroxyl group, we tested this assumption out of the infinite dilution limits by representing the phase behavior of CO_2 + methanol binary systems, using different values of M_{CO2} but keeping the product $M_{CO2} \times \kappa_{cross}$ constant (3.0432 cm^3/mol). Particularly, we compared the previous results with M_{CO2} = 2 and κ_{cross} = 1.521 cm^3/mol and a new set M_{CO2} = 8 and κ_{cross} = 0.3804 cm^3/mol, respectively.

Figure 10 depicts VLE of CO_2 + methanol binary system setting the number of association sites in 2 and 8; note that both cases show almost the same behavior, also out of the infinite dilution limits. In addition, we also checked that the GCA-EOS shows the same results for any other values of M_{CO2}, between 2 and 8 (not shown in the figure).

4. CONCLUSIONS

It is well-known that VLE and LLE experimental data are needed to train semiempirical thermodynamic models. However, the overall phase behavior and critical loci of binary systems are also key information, especially in mixtures showing multiphase equilibria, such it is the case of systems containing CO_2.

This paper reports the second part of an extensive work of thoroughly modeling the phase behavior of CO_2 with homologous families of organic compounds. In Part I we assessed the complex CO_2 + hydrocarbons binary systems comprising hydrocarbons

DOI: 10.1021/acs.jced.7b00663
J. Chem. Eng. Data XXXX, XXX, XXX−XXX

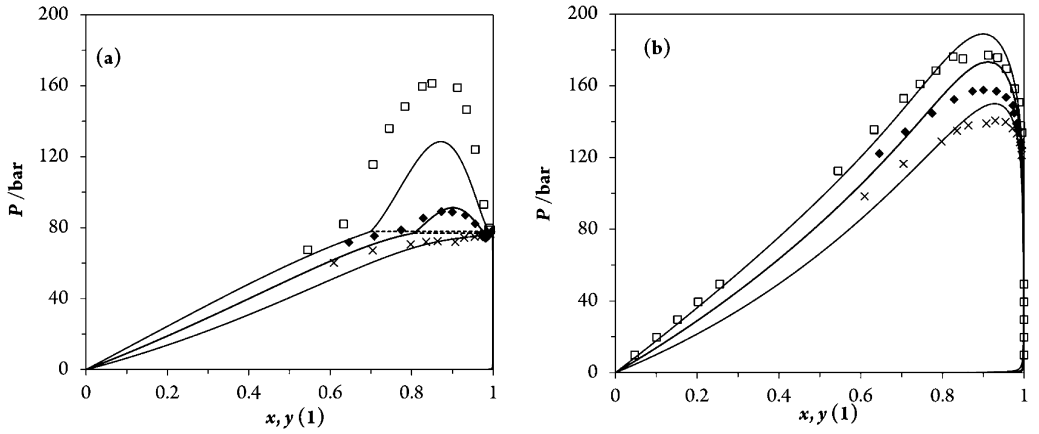

Figure 9. Phase equilibria of CO_2 (1) + octanol isomers binary systems at (a) 308 K (b) 348 K: (×) 2,2,4-trimethyl-1-pentanol; (♦) 2-ethyl-1-hexanol; and (□) 1-octanol. Symbols: experimental data[25,103] Solid lines: GCA-EOS predictions.

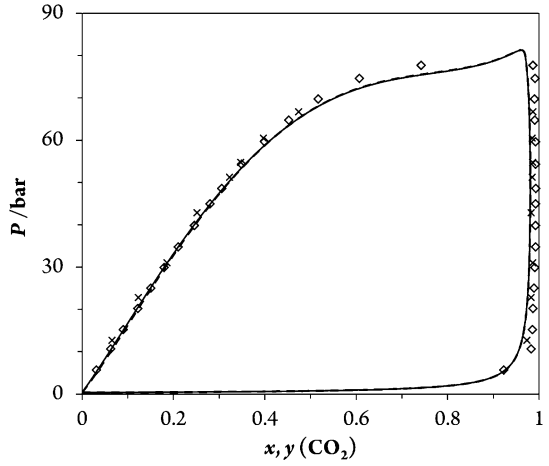

Figure 10. Performance of GCA-EoS with different number of electropositive sites in the CO_2 molecule (M_{CO2}) in the binary system CO_2 + methanol at 313 K but keeping the product $M_{CO2} \times \kappa_{cross}$ constant. Symbols: experimental data.[55,60] Solid line: $M_{CO2} = 2$ and $\kappa_{cross} = 1.521$ cm^3/mol. Dashed line: $M_{CO2} = 8$ and $\kappa_{cross} = 0.3804$ cm^3/mol.

up to hexatriacontane. This follow-up work shows that the GCA-EOS is also able to correlate and predict the binary systems of CO_2 with the homologues family of alcohols. The experimental database covers binary systems of CO_2 + linear and branched alcohols up to 1-hexadecanol, temperatures from 230 to 573 K, and pressures up to 400 bar. Special emphasis was set on the search of parameters that allow accurate representation of saturation and critical points simultaneously; thus, also the type of binary phase behavior is attained.

Several authors have shown experimental evidence of the formation of weak electron donor−electron acceptor complexes between CO_2 and alcohols. This was taken into account in the parametrization procedure by allowing cross association between the hydroxyl group and two electropositive sites in the CO_2 molecule. Furthermore, we have shown that for a weak solvation interaction, the number of positive sites in the CO_2 molecule can be set arbitrarily, as far as the product of the number of association sites and cross association volume is kept constant.

In this work, we only parametrized the residual binary interaction and solvation parameters between CO_2 and the alcohol group, since in Part I of this work the interaction between CO_2 and alkyl chains was addressed. We modeled almost 30 alcohols based on 6 new parameters, which come from the correlation of only 3 alcohols in binary systems with CO_2. This result shows that the previous parametrizations of GCA-EOS are robust, since most of the parameters come from past works and none of them required refitting. The whole set correctly represents the transformation of the type of phase behavior of the CO_2 + *n*-alcohols homologous series, as the alcohol alkyl chain increases. In addition, the GCA-EOS is also able to quantitatively predict phase behavior of CO_2 + branched alcohols and describe binary excess properties, as expected since the parametrization covers a wide range of conditions.

APPENDIX: THE GCA-EOS MODEL

There are three contributions to the residual Helmholtz energy (A^R) in the GCA-EoS model:[138] free volume (A^{fv}), attractive (A^{att}), and association (A^{assoc}).

$$A^R = A^{fv} + A^{att} + A^{assoc} \tag{A.1}$$

The free volume contribution is represented by the extended Carnahan−Starling[35] equation for mixtures of hard spheres developed by Mansoori and Leland:[139]

$$\frac{A^{fv}}{RT} = 3\frac{\lambda_1\lambda_2}{\lambda_3}(Y-1) + \frac{\lambda_2^3}{\lambda_3^2}(Y^2 - Y - \ln Y) + n \ln Y \tag{A.2}$$

with

$$Y = \left(1 - \frac{\pi\lambda_3}{6V}\right)^{-1} \tag{A.3}$$

$$\lambda_k = \sum_{i=1}^{NC} n_i d_i^k \quad (k = 1, 2, 3) \tag{A.4}$$

where n_i is the number of moles of component *i*, NC stands for the number of components, V represents the total volume, R stands for the universal gas constant, T is temperature, and d_i the hard-sphere diameter per mole of species *i*.

The following generalized expression gives the temperature dependence of the hard sphere diameter:

$$d_i = 1.065655 d_{ci}\left[1 - 0.12 \exp\left(\frac{-2T_{ci}}{3T}\right)\right] \tag{A.5}$$

where d_{ci} and T_{ci} are, respectively, the critical hard-sphere diameter and critical temperature of component *i*.

DOI: 10.1021/acs.jced.7b00663
J. Chem. Eng. Data XXXX, XXX, XXX−XXX

The attraction contribution to the residual Helmholtz energy, A^{att}, accounts for dispersive forces between functional groups. It is a van der Waals expression combined with a density-dependent local-composition mixing rule based on a group contribution version of the NRTL model.[36] The van der Waals expression for the attractive Helmholtz energy is equal to $-a{\cdot}n{\cdot}\rho$, for which a is the energy parameter, n is the number of moles, and ρ is the mole density. For a pure component, a is computed as follows:

$$a = \frac{z}{2} q^2 g \tag{A.6}$$

where g is the characteristic attractive energy per segment and q is the number of surface segments as defined in the UNIFAC method.[140] The interactions are assumed to take place through the surface and the coordination number (z) is set equal to 10 as usual.[140] In GCA-EoS the extension to mixtures is carried out using the NRTL model, but using local surface fractions such as in UNIQUAC[141] rather than local mole fractions:

$$\frac{A^{att}}{RT} = -\frac{\frac{z}{2}\tilde{q}^2 g_{mix}}{RTV} \tag{A.7}$$

where $\tilde{q}$ is the total number of surface segments and g_{mix} is the mixture characteristic attraction energy per total segments and are calculated as follows:

$$g_{mix} = \sum_{i=1}^{NG} \theta_i \sum_{j=1}^{NG} \frac{\theta_j \tau_{ji} g_{ji}}{\sum_{k=1}^{NG} \theta_k \tau_{ki}} \tag{A.8}$$

and

$$\tilde{q} = \sum_{i=1}^{NC} \sum_{j=1}^{NG} n_i \nu_{ij} q_j \tag{A.9}$$

where ν_{ij} is the number of groups of type j in molecule i; q_j stands for the number of surface segments assigned to group j, θ_j represents the surface fraction of group j

$$\theta_j = \frac{1}{\tilde{q}} \sum_{i=1}^{NC} n_i \nu_{ij} q_j \tag{A.10}$$

$$\tau_{ij} = \exp\left(\alpha_{ij} \frac{\tilde{q} \Delta g_{ij}}{RTV}\right) \tag{A.11}$$

$$\Delta g_{ij} = g_{ij} - g_{jj} \tag{A.12}$$

g_{ij} is the attractive energy between groups i and j, and α_{ij} is the nonrandomness parameter. It is worth highlighting that, in the absence of nonrandomness ($\alpha_{ij} = 0$), eq A.8 gives the classical quadratic mixing rule.

The attractive energy, g_{ij}, is calculated from the energy between like-group segments through the following combination rule:

$$g_{ij} = k_{ij}\sqrt{g_{ii} g_{jj}} \quad (k_{ij} = k_{ji}) \tag{A.14}$$

with the following temperature dependence for the energy and interaction parameters:

$$g_{ii} = g_{ii}^*\left[1 + g_{ii}'\left(\frac{T}{T_i^*} - 1\right) + g_{ii}'' \ln\left(\frac{T}{T_i^*}\right)\right] \tag{A.15}$$

and

$$k_{ij} = k_{ij}^*\left[1 + k_{ij}' \ln\left(\frac{2T}{T_i^* + T_j^*}\right)\right] \tag{A.16}$$

where g_{ii}^* is the attraction energy and k_{ij}^* the interaction parameter at the reference temperature T_i^* and $(T_i^* + T_j^*)/2$, respectively.

Finally, the association term,[138] A^{assoc}, is a group contribution version of the SAFT equation of Chapman et al.:[37]

$$\frac{A^{assoc}}{RT} = \sum_{i=1}^{NGA} n_i^*\left[\sum_{k=1}^{M_i}\left(\ln X_{ki} - \frac{X_{ki}}{2}\right) + \frac{M_i}{2}\right] \tag{A.17}$$

In this equation NGA represents the number of associating functional groups, n_i^* is the total number of moles of associating group i, X_{ki} is the fraction of group i nonbonded through site k, and M_i is the number of associating sites in group i. The total number of moles of associating group i is calculated from the number ν_{mi}^* of associating groups i present in molecule m and the total amount of moles of specie m (n_m):

$$n_i^* = \sum_{m=1}^{NC} \nu_{mi}^* n_m \tag{A.18}$$

The fraction of groups i nonbonded through site k is determined by the expression:

$$X_{ki} = \left(1 + \sum_{j=1}^{NGA} \sum_{l=1}^{M_j} \frac{n_j^* X_{lj} \Delta_{ki,lj}}{V}\right)^{-1} \tag{A.19}$$

where the summation includes all NGA associating groups and M_j sites. X_{ki} depends on the association strength, $\Delta_{ki.lj}$:

$$\Delta_{ki.lj} = \kappa_{ki.lj}\left[\exp\left(\frac{\varepsilon_{ki,lj}}{RT}\right) - 1\right] \tag{A.20}$$

The association strength between site k of group i and site l of group j depends on the temperature T and on the association parameters $\kappa_{ki,jl}$ and $\varepsilon_{ki,jl}$, which represent the volume and energy of association, respectively.

AUTHOR INFORMATION

Corresponding Author

*E-mail: spereda@plapiqui.edu.ar.

ORCID

Selva Pereda: 0000-0002-2320-4298

Funding

The authors acknowledge the financial support granted by the Consejo Nacional de Investigaciones Científicas y Técnicas (PIP 112 2015 010 856), the Ministerio de Ciencia, Tecnología e Innovación Productiva (PICT 2016-0907), and Universidad Nacional del Sur (PGI - 24/M133).

Notes

The authors declare no competing financial interest.

LIST OF SYMBOLS

A	Helmholtz free energy
ARD(Z)	absolute relative deviation $\left\lvert 1 - \frac{Z_{calci}}{Z_{expi}} \right\rvert$
AAD(Z)	average absolute deviation in variable Z: $\frac{1}{N}\sum_i^N \lvert Z_{expi} - Z_{calci} \rvert$

DOI: 10.1021/acs.jced.7b00663
J. Chem. Eng. Data XXXX, XXX, XXX−XXX

AARD(Z)%	average absolute relative deviation in variable Z: $\frac{100}{N}\sum_i^N \left\lvert 1 - \frac{Z_{calci}}{Z_{expi}} \right\rvert$
CN	carbon number
d_{ci}	effective hard sphere diameter of component i evaluated at T_c
g_j	group energy per surface segment of group j
EDA	electron donor−acceptor
LLE	liquid−liquid equilibria
N	number of experimental points of each data set
NC	number of components in the mixture
NG	number of attractive groups in the mixture
NGA	number of associating groups in the mixture
M_i	Total number of associating sites in group i
P	pressure
q_j	number of surface segments of group j
R	universal gas constant
SFLE	supercritical fluid-liquid equilibria
T	temperature
T_{ci}	critical temperature of component i
V	total volume of the mixture
VLE	vapor−liquid equilibria
w_i	mass composition of component i
X_{ki}	fraction of nonbonded associating sites of type k in group i
x_i	molar composition in liquid phase of component i
y_i	molar composition in vapor phase of component i
Z	dummy variable

Greek Symbols

α_{ij}	nonrandomness parameter between groups i and j
ΔZ%	AARD% in variable Z
$\Delta_{ki,lj}$	association strength between site k of group i and site l of group j
$\varepsilon_{ki,lj}$	energy of association between site k of group i and site l of group j
$\kappa_{ki,lj}$	volume of association between site k of group i and site l of group j
ν_{ij}^*	number of associating groups j in compound i
$\hat{\varphi}_i$	fugacity coefficient of compound i in the mixture

REFERENCES

(1) González Prieto, M.; Sánchez, F. A.; Pereda, S. Multiphase Equilibria Modeling with GCA-EoS. Part I: Carbon Dioxide with the Homologous Series of Alkanes up to 36 Carbons. *Ind. Eng. Chem. Res.* **2015**, *54*, 12415−12427.

(2) Peters, C. J.; Gauter, K. Occurrence of Holes in Ternary Fluid Multiphase Systems of Near-Critical Carbon Dioxide and Certain Solutes. *Chem. Rev.* **1999**, *99*, 419−432.

(3) van Konynenburg, P. H.; Scott, R. L. Critical Lines and Phase Equilibria in Binary Van Der Waals Mixtures. *Philos. Trans. R. Soc., A* **1980**, *298*, 495−540.

(4) Peters, C. J.; Lichtenthaler, R. N.; de Swaan Arons, J. Three Phase Equilibria in Binary Mixtures of Ethane and Higher N-Alkanes. *Fluid Phase Equilib.* **1986**, *29*, 495−504.

(5) Peters, C. J.; de Swaan Arons, J.; Levelt Sengers, J. M. H.; Gallagher, J. S. Global Phase Behavior of Mixtures of Short and Long *n*-Alkanes. *AIChE J.* **1988**, *34*, 834−839.

(6) Peters, C. J.; van der Kooi, H. J.; De Roo, J. L.; de Swaan Arons, J.; Gallagher, J. S.; Levelt Sengers, J. M. H. The Search for Tricriticality in Binary Mixtures of near-Critical Propane and Normal Paraffins. *Fluid Phase Equilib.* **1989**, *51*, 339−351.

(7) Peters, C. J.; de Swaan Arons, J.; Harvey, A. H.; Levelt Sengers, J. M. H. On the Relationship between the Carbon-Number of *n*-Paraffins and Their Solubility in Supercritical Solvents. *Fluid Phase Equilib.* **1989**, *52*, 389−396.

(8) Peters, C. J. Multiphase Equilibria in Near-Critical Solvents. In *Supercritical Fluids*; Kiran, E., Levelt Sengers, J. M. H., Eds.; Springer Netherlands: Dordrecht, 1994; pp 117−145.

(9) Peters, C. J.; Florusse, L. J.; Hähre, S.; de Swaan Arons, J. Fluid Multiphase Equilibria and Critical Phenomena in Binary and Ternary Mixtures of Carbon Dioxide, Certain *n*-Alkanols and Tetradecane. *Fluid Phase Equilib.* **1995**, *110*, 157−173.

(10) Raeissi, S.; Gauter, K.; Peters, C. J. Fluid Multiphase Behavior in Quasi-Binary Mixtures of Carbon Dioxide and Certain 1-Alkanols. *Fluid Phase Equilib.* **1998**, *147*, 239−249.

(11) Brunner, G. *Gas Extraction*; Topics in Physical Chemistry; Baumgärtel, H., Franck, E. U., Grünbein, W., Eds.; Springer-Verlag Berlin Heilderberg GmbH: Heidelberg, 1994; Vol. *4*.

(12) Wong, J. M.; Johnston, K. P. Solubilization of Biomolecules in Carbon Dioxide Based Supercritical Fluids. *Biotechnol. Prog.* **1986**, *2*, 29−39.

(13) *High Pressure Fluid Technology for Green Food Processing*, 1st ed.; Food Engineering Series; Fornari, T., Stateva, R. P., Eds.; Springer International Publishing: Cham, 2015.

(14) Sloan, E. D. *Clathrate Hydrates of Natural Gases*, 2nd ed.; Marcel Dekker, Inc.: New York, 1998.

(15) Sloan, E. D. Fundamental Principles and Applications of Natural Gas Hydrates. *Nature* **2003**, *426*, 353−363.

(16) Pereda, S. Ingeniería del equilibrio entre fases: Aplicación a reactores de hidrogenación supercrítica (Phase balance engineering: Application to supercritical hydrogenation reactors). Ph.D. Thesis, Universidad Nacional del Sur, Bahía Blanca, Argentina, 2003.

(17) Oliveira, M. B.; Queimada, A. J.; Kontogeorgis, G. M.; Coutinho, J. A. P. Evaluation of the CO_2 Behavior in Binary Mixtures with Alkanes, Alcohols, Acids and Esters Using the Cubic-Plus-Association Equation of State. *J. Supercrit. Fluids* **2011**, *55*, 876−892.

(18) Tsivintzelis, I.; Kontogeorgis, G. M.; Michelsen, M. L.; Stenby, E. H. Modeling Phase Equilibria for Acid Gas Mixtures Using the CPA Equation of State. Part II: Binary Mixtures with CO_2. *Fluid Phase Equilib.* **2011**, *306*, 38−56.

(19) Grenner, A.; Kontogeorgis, G. M.; von Solms, N.; Michelsen, M. L. Modeling Phase Equilibria of Alkanols with the Simplified PC-SAFT Equation of State and Generalized Pure Compound Parameters. *Fluid Phase Equilib.* **2007**, *258*, 83−94.

(20) Hsieh, C.-M.; Windmann, T.; Vrabec, J. Vapor−Liquid Equilibria of CO_2 + C_1−C_5 Alcohols from the Experiment and the COSMO-SAC Model. *J. Chem. Eng. Data* **2013**, *58*, 3420−3429.

(21) Kolář, P.; Kojima, K. Prediction of Critical Points in Multicomponent Systems Using the PSRK Group Contribution Equation of State. *Fluid Phase Equilib.* **1996**, *118*, 175−200.

(22) Li, X.; Englezos, P. Vapor - Liquid Equilibrium of Systems Containing Alcohols Using the Statistical Associating Fluid Theory Equation of State. *Ind. Eng. Chem. Res.* **2003**, *42*, 4953−4961.

(23) Li, X.-S.; Englezos, P. Vapor−liquid Equilibrium of Systems Containing Alcohols, Water, Carbon Dioxide and Hydrocarbons Using SAFT. *Fluid Phase Equilib.* **2004**, *224*, 111−118.

(24) Tsivintzelis, I.; Ali, S.; Kontogeorgis, G. M. Modeling Phase Equilibria for Acid Gas Mixtures Using the CPA Equation of State. Part IV. Applications to Mixtures of CO_2 with Alkanes. *Fluid Phase Equilib.* **2015**, *397*, 1−17.

(25) Schwarz, C. E.; Fourie, F. C. v. N.; Knoetze, J. H. Phase Equilibria of Alcohols in Supercritical Fluids Part II. The Effect of Side Branching on C_8 Alcohols in Supercritical Carbon Dioxide. *J. Supercrit. Fluids* **2009**, *51*, 128−135.

(26) Zamudio, M.; Schwarz, C. E.; Knoetze, J. H. Phase Equilibria of Branched Isomers of C_{10}-Alcohols and C_{10}-Alkanes in Supercritical Carbon Dioxide. *J. Supercrit. Fluids* **2011**, *59*, 14−26.

(27) Polishuk, I.; Wisniak, J.; Segura, H. Simultaneous Prediction of the Critical and Sub-Critical Phase Behavior in Mixtures Using Equation of State I. Carbon Dioxide-Alkanols. *Chem. Eng. Sci.* **2001**, *56*, 6485−6510.

DOI: 10.1021/acs.jced.7b00663
J. Chem. Eng. Data XXXX, XXX, XXX−XXX

(28) Llovell, F.; Vega, L. F. Global Fluid Phase Equilibria and Critical Phenomena of Selected Mixtures Using the Crossover Soft-SAFT Equation. *J. Phys. Chem. B* **2006**, *110*, 1350−1362.
(29) Gregg, C. J.; Stein, F. P.; Radosz, M. Phase Behavior of Telechelic Polyisobutylene in Subcritical and Supercritical Fluids. 4. SAFT Association Parameters from FTIR for Blank, Monohydroxy, and Dihydroxy PIB 200 in Ethane, Carbon Dioxide, and Chlorodifluoromethane. *J. Phys. Chem. B* **1999**, *103*, 1167−1175.
(30) Huang, S. H.; Radosz, M. Equation of State for Small, Large, Polydisperse, and Associating Molecules: Extension to Fluid Mixtures. *Ind. Eng. Chem. Res.* **1991**, *30*, 1994−2005.
(31) Nguyen-Huynh, D.; Passarello, J.-P.; de Hemptinne, J.-C.; Volle, F.; Tobaly, P. Simultaneous Modeling of VLE, LLE and VLLE of CO_2 and 1, 2, 3 and 4 Alkanol Containing Mixtures Using GC-PPC-SAFT EOS. *J. Supercrit. Fluids* **2014**, *95*, 146−157.
(32) Nguyen-Huynh, D.; Passarello, J.-P.; Tobaly, P.; de Hemptinne, J.-C. Modeling Phase Equilibria of Asymmetric Mixtures Using a Group-Contribution SAFT (GC-SAFT) with a Kij Correlation Method Based on London's Theory. 1. Application to CO_2 + *n*-Alkane, Methane + *n*-Alkane, and Ethane + *n*-Alkane Systems Dong. *Ind. Eng. Chem. Res.* **2008**, *47*, 8847−8858.
(33) Fulton, J. L.; Yee, G. G.; Smith, R. D. Hydrogen Bonding of Simple Alcohols in Supercritical Fluids; ACS Symposium Series 514; Kiran, E., Brennecke, J. F., Eds.; American Chemical Society: Washington, DC, 1992; pp 175−187.
(34) Bjørner, M. G.; Kontogeorgis, G. M. Modelling the Phase Equilibria of Multicomponent Mixtures Containing CO2, Alkanes, Water, And/or Alcohols Using the Quadrupolar CPA Equation of State. *Mol. Phys.* **2016**, *114*, 2641−2654.
(35) Carnahan, N. F.; Starling, K. E. Equation of State for Nonattracting Rigid Spheres. *J. Chem. Phys.* **1969**, *51*, 635.
(36) Renon, H.; Prausnitz, J. M. Local Compositions in Thermodynamic Excess Functions for Liquid Mixtures. *AIChE J.* **1968**, *14*, 135−144.
(37) Chapman, W. G.; Gubbins, K. E.; Jackson, G.; Radosz, M. SAFT: Equation-of-State Solution Model for Associating Fluids. *Fluid Phase Equilib.* **1989**, *52*, 31−38.
(38) Hemmaplardh, B.; King, A. D., Jr. Solubility of Methanol in Compressed Nitrogen, Argon, Methane, Ethylene, Ethane, Carbon Dioxide, and Nitrous Oxide. Evidence for Association of Carbon Dioxide with Methanol in the Gas Phase. *J. Phys. Chem.* **1971**, *76*, 2170−2175.
(39) Coan, C. R.; King, A. D., Jr. Solubility of Water in Compressed Carbon Dioxide, Nitrous Oxide, and Ethane. Evidence for Hydration of Carbon Dioxide and Nitrous Oxide in the Gas Phase. *J. Am. Chem. Soc.* **1971**, *93*, 1857−1862.
(40) Gupta, S. K.; Lesslie, R. D.; King, A. D., Jr. Solubility of Alcohols in Compressed Gases. A Comparison of Vapor-Phase Interactions of Alcohols and Homomorphic Compounds with Various Gases. 1. Ethanol in Compressed Helium, Hydrogen, Argon, Methane, Ethylene, Ethane, Carbon Dioxide, and Nitrous Oxide. *J. Phys. Chem.* **1973**, *77*, 2011−2015.
(41) Cox, A. J.; Ford, T. A.; Glasser, L. Ab Initio Molecular Orbital Calculations of the Infrared Spectra of Interacting Water Molecules. Part 4. Interaction Energies and Band Intensities of the Complexes of Water with Carbon Dioxide and Nitrous Oxide. *J. Mol. Struct.: THEOCHEM* **1994**, *312*, 101−108.
(42) Danten, Y.; Tassaing, T.; Besnard, M. Vibrational Spectra of CO_2-Electron Donor-Acceptor Complexes from Ab Initio. *J. Phys. Chem. A* **2002**, *106*, 11831−11840.
(43) Saharay, M.; Balasubramanian, S. Electron Donor-Acceptor Interactions in Ethanol-CO_2 Mixtures: An Ab Initio Molecular Dynamics Study of Supercritical Carbon Dioxide. *J. Phys. Chem. B* **2006**, *110*, 3782−3790.
(44) Xu, W.; Yang, J.; Hu, Y. Microscopic Structure and Interaction Analysis for Supercritical Carbon Dioxide-Ethanol Mixtures: A Monte Carlo Simulation Study. *J. Phys. Chem. B* **2009**, *113*, 4781−4789.
(45) Soria, T. M.; Andreatta, A. E.; Pereda, S.; Bottini, S. B. Thermodynamic Modeling of Phase Equilibria in Biorefineries. *Fluid Phase Equilib.* **2011**, *302*, 1−9.
(46) Secuianu, C.; Feroiu, V.; Geană, D. High-Pressure Vapor-Liquid Equilibria in the System Carbon Dioxide + 1-Butanol at Temperatures from (293.15 to 324.15) K. *J. Chem. Eng. Data* **2004**, *49*, 1635−1638.
(47) Elizalde-Solis, O.; Galicia-Luna, L. A.; Camacho-Camacho, L. E. High-Pressure Vapor−liquid Equilibria for CO_2+alkanol Systems and Densities of *n*-Dodecane and *n*-Tridecane. *Fluid Phase Equilib.* **2007**, *259*, 23−32.
(48) Secuianu, C.; Feroiu, V.; Geană, D. High-Pressure Phase Equilibria in the (Carbon dioxide+1-Hexanol) System. *J. Chem. Thermodyn.* **2010**, *42*, 1286−1291.
(49) Secuianu, C.; Feroiu, V.; Geană, D. High-Pressure Vapor−liquid and Vapor−liquid−liquid Equilibria in the Carbon dioxide+1-Heptanol System. *Fluid Phase Equilib.* **2008**, *270*, 109−115.
(50) Soria, T. M.; Sánchez, F. A.; Pereda, S.; Bottini, S. B. Modeling Alcohol+water+hydrocarbon Mixtures with the Group Contribution with Association Equation of State GCA-EoS. *Fluid Phase Equilib.* **2010**, *296*, 116−124.
(51) Design Institute for Physical Properties, *Project 801: Evaluated Process Design Data, American Institute of Chemical Engineers*; Design Institute for Physical Property Research: New York, 1998.
(52) Nikitin, E. D.; Popov, A. P.; Bogatishcheva, N. S.; Kuznetsov, V. A. Critical Temperatures and Pressures of Straight-Chain Alkanediols (C_3 to C_{12}). *Fluid Phase Equilib.* **2013**, *355*, 40−45.
(53) Skjold-Jørgensen, S. Group Contribution Equation of State (GC-EOS): A Predictive Method for Phase Equilibrium Computations over Wide Ranges of Temperature and Pressures up to 30 MPa. *Ind. Eng. Chem. Res.* **1988**, *27*, 110−118.
(54) Fonseca, J. M. S.; Dohrn, R.; Peper, S. High-Pressure Fluid-Phase Equilibria: Experimental Methods and Systems Investigated (2005−2008). *Fluid Phase Equilib.* **2011**, *300*, 1−69.
(55) Naidoo, P.; Ramjugernath, D.; Raal, J. D. A New High-Pressure Vapour−liquid Equilibrium Apparatus. *Fluid Phase Equilib.* **2008**, *269*, 104−112.
(56) Hong, J. H.; Kobayashi, R. Vapor Liquid Equilibrium Studies for the Carbon Dioxide-Methanol System. *Fluid Phase Equilib.* **1988**, *41*, 269−276.
(57) Brunner, E.; Hültenschmidt, W.; Schlichthärle, G. Fluid Mixtures at High Pressures IV. Isothermal Phase Equilibria in Binary Mixtures Consisting of (Methanol + Hydrogen or Nitrogen or Methane or Carbon Monoxide or Carbon Dioxide). *J. Chem. Thermodyn.* **1987**, *19*, 273−291.
(58) Secuianu, C.; Feroiu, V.; Geană, D. Phase Behavior for Carbon Dioxide+ethanol System: Experimental Measurements and Modeling with a Cubic Equation of State. *J. Supercrit. Fluids* **2008**, *47*, 109−116.
(59) Tian, Y.-L.; Han, M.; Chen, L.; Feng, J.-J.; Qin, Y. Study on Vapor-Liquid Phase Equilibria for CO_2-C_2H_5OH System (in Chinise). *Acta Physico-Chimica Sin.* **2001**, *17*, 155−160.
(60) Tochigi, K.; Namae, T.; Suga, T.; Matsuda, H.; Kurihara, K.; dos Ramos, M. C.; McCabe, C. Measurement and Prediction of High-Pressure Vapor−liquid Equilibria for Binary Mixtures of Carbon Dioxide+*n*-Octane, Methanol, Ethanol, and Perfluorohexane. *J. Supercrit. Fluids* **2010**, *55*, 682−689.
(61) Schwinghammer, S.; Siebenhofer, M.; Marr, R. Determination and Modelling of the High-Pressure Vapour−liquid Equilibrium Carbon Dioxide−methyl Acetate. *J. Supercrit. Fluids* **2006**, *38*, 1−6.
(62) Joung, S. N.; Yoo, C. W.; Shin, H. Y.; Kim, S. Y.; Yoo, K.-P.; Lee, C. S.; Huh, W. S. Measurements and Correlation of High-Pressure VLE of Binary CO_2−alcohol Systems (Methanol, Ethanol, 2-Methoxyethanol and 2-Ethoxyethanol). *Fluid Phase Equilib.* **2001**, *185*, 219−230.
(63) Suzuki, K.; Sue, H.; Itou, M.; Smith, R. L.; Inomata, H.; Arai, K.; Saito, S. Isothermal Vapor-Liquid Equilibrium Data for Binary Systems at High Pressures: Carbon Dioxide-Methanol, Carbon Dioxide-Ethanol, Carbon Dioxide-1-Propanol, Methane-Ethanol, Methane-1-Propanol, Ethane-Ethanol, and Ethane-1-Propanol Systems. *J. Chem. Eng. Data* **1990**, *35*, 63−66.

DOI: 10.1021/acs.jced.7b00663
J. Chem. Eng. Data XXXX, XXX, XXX−XXX

(64) Bezanehtak, K.; Combes, G. B.; Dehghani, F.; Foster, N. R.; Tomasko, D. L. Vapor - Liquid Equilibrium for Binary Systems of Carbon Dioxide + Methanol, Hydrogen + Methanol, and Hydrogen + Carbon Dioxide at High Pressures. *J. Chem. Eng. Data* **2002**, *47*, 161−168.
(65) Ohgaki, K.; Katayama, T. Isothermal Vapor-Liquid Equilibrium Data for Binary Systems Containing Carbon Dioxide at High Pressures: Methanol-Carbon Dioxide, N-Hexane-Carbon Dioxide, and Benzene-Carbon Dioxide Systems. *J. Chem. Eng. Data* **1976**, *21*, 53−55.
(66) Leu, A.-D.; Chung, S. Y.-K.; Robinson, D. B. The Equilibrium Phase Properties of (Carbon Dioxide + Methanol). *J. Chem. Thermodyn.* **1991**, *23*, 979−985.
(67) Chang, C. J.; Chiu, K.-L.; Day, C.-Y. A New Apparatus for the Determination of *P*−*x*−*y* Diagrams and Henry's Constants in High Pressure Alcohols with Critical Carbon Dioxide. *J. Supercrit. Fluids* **1998**, *12*, 223−237.
(68) Elbaccouch, M. M.; Raymond, M. B.; Elliott, J. R. High-Pressure Vapor - Liquid Equilibrium for R-22 + Ethanol and R-22 + Ethanol + Water. *J. Chem. Eng. Data* **2000**, *45*, 280−287.
(69) Laursen, T.; Rasmussen, P.; Andersen, S. I. VLE and VLLE Measurements of Dimethyl Ether Containing Systems. *J. Chem. Eng. Data* **2002**, *47*, 198−202.
(70) Chang, T.; Rousseau, R. W. Solubilities of Carbon Dioxide in Methanol and Methanol-Water at High Pressures: Experimental Data and Modeling. *Fluid Phase Equilib.* **1985**, *23*, 243−258.
(71) Kariznovi, M.; Nourozieh, H.; Abedi, J. Experimental Measurements and Predictions of Density, Viscosity, and Carbon Dioxide Solubility in Methanol, Ethanol, and 1-Propanol. *J. Chem. Thermodyn.* **2013**, *57*, 408−415.
(72) Kodama, D.; Kato, M. High-Pressure Phase Equilibrium for Carbon Dioxide + Ethanol at 291.15 K. *J. Chem. Eng. Data* **2005**, *50*, 16−17.
(73) Pfohl, O.; Pagel, A.; Brunner, G. Phase Equilibria in Systems Containing *o*-Cresol, *p*-Cresol, Carbon Dioxide, and Ethanol at 323.15−473.15 K and 10−35 MPa. *Fluid Phase Equilib.* **1999**, *157*, 53−79.
(74) Jennings, D. W.; Lee, R.-J.; Teja, A. S. Vapor-Liquid Equilibria in the Carbon Dioxide + Ethanol and Carbon Dioxide + 1-Butanol Systems. *J. Chem. Eng. Data* **1991**, *36*, 303−307.
(75) Galicia-luna, L. A.; Ortega-Rodríguez, A.; Richon, D. New Apparatus for the Fast Determination of High-Pressure Vapor - Liquid Equilibria of Mixtures and of Accurate Critical Pressures. *J. Chem. Eng. Data* **2000**, *45*, 265−271.
(76) Yoon, J.; Lee, H.-S.; Lee, H. High-Pressure Vapor-Liquid Equilibria for Carbon Dioxide + Methanol, Carbon Dioxide + Ethanol, and Carbon Dioxide + Methanol + Ethanol. *J. Chem. Eng. Data* **1993**, *38*, 53−55.
(77) Lim, J. S.; Lee, Y. Y.; Chun, H. S. Phase Equilibria for Carbon Dioxide-Ethanol-Water System at Elevated Pressures. *J. Supercrit. Fluids* **1994**, *7*, 219−230.
(78) Tsivintzelis, I.; Missopolinou, D.; Kalogiannis, K.; Panayiotou, C. Phase Compositions and Saturated Densities for the Binary Systems of Carbon Dioxide with Ethanol and Dichloromethane. *Fluid Phase Equilib.* **2004**, *224*, 89−96.
(79) Hirohama, S.; Takatsuka, T.; Miyamoto, S.; Muto, T. Measurement and Correlation of Phase Equilibria for the Carbon Dioxide-Ethanol-Water System. *J. Chem. Eng. Jpn.* **1993**, *26*, 408−415.
(80) Stievano, M.; Elvassore, N. High-Pressure Density and Vapor−liquid Equilibrium for the Binary Systems Carbon Dioxide−ethanol, Carbon Dioxide−acetone and Carbon Dioxide−dichloromethane. *J. Supercrit. Fluids* **2005**, *33*, 7−14.
(81) Sima, S.; Feroiu, V.; Geană, D. New High Pressure Vapor−Liquid Equilibrium and Density Predictions for the Carbon Dioxide + Ethanol System. *J. Chem. Eng. Data* **2011**, *56*, 5052−5059.
(82) Gutiérrez, J. E.; Bejarano, A.; Fuente, J. C. D. La. Measurement and Modeling of High-Pressure (Vapour+liquid) Equilibria of (CO_2+alcohol) Binary Systems. *J. Chem. Thermodyn.* **2010**, *42*, 591−596.
(83) Secuianu, C.; Feroiu, V.; Geană, D. High-Pressure Phase Equilibria for the Carbon Dioxide + 1-Propanol System. *J. Chem. Eng. Data* **2008**, *53*, 2444−2448.
(84) Vandana, V.; Teja, A. S. Vapor-Liquid Equilibria in the Carbon Dioxide + 1-Propanol System. *J. Chem. Eng. Data* **1995**, *40*, 459−461.
(85) Hiaki, T.; Miyagi, H.; Tsuji, T.; Hongo, M. Vapor−liquid Equilibria for Supercritical Carbon Dioxide+butanol Systems at 313.2 K. *J. Supercrit. Fluids* **1998**, *13*, 23−27.
(86) Ishihara, K.; Tsukajima, A.; Tanaka, H.; Kato, M.; Sako, T.; Sato, M.; Hakuta, T. Vapor - Liquid Equilibrium for Carbon Dioxide + 1-Butanol at High Pressure. *J. Chem. Eng. Data* **1996**, *41*, 324−325.
(87) Borch-Jensen, C.; Staby, A.; Mollerup, J. M. Mutual Solubility of 1-Butanol and Carbon Dioxide, Ethene, Ethane, or Propane at a Reduced Supercritical Solvent Temperature of 1.03. *J. Supercrit. Fluids* **1994**, *7*, 231−244.
(88) Silva-Oliver, G.; Galicia-luna, L. A. Vapor−liquid Equilibria near Critical Point and Critical Points for the CO_2 + 1-Butanol and CO_2 + 2-Butanol Systems at Temperatures from 324 to 432 K. *Fluid Phase Equilib.* **2001**, *182*, 145−156.
(89) Chen, H.-I.; Chang, H.-Y.; Chen, P.-H. High-Pressure Phase Equilibria of Carbon Dioxide + 1-Butanol, and Carbon Dioxide + Water + 1-Butanol Systems. *J. Chem. Eng. Data* **2002**, *47*, 776−780.
(90) Jennings, D. W.; Chang, F.; Bazaan, V.; Teja, A. S. Vapor-Liquid Equilibria for Carbon Dioxide + 1-Pentanol. *J. Chem. Eng. Data* **1992**, *37*, 337−338.
(91) Secuianu, C.; Feroiu, V.; Geană, D. High-Pressure Vapour-Liquid Equilibria of Carbon Dioxide+ 1-Pentanol System-Experimental Measurements and Modelling. *Rev. Chim.* **2007**, *58*, 1176−1181.
(92) Secuianu, C.; Feroiu, V.; Geană, D. Measurements and Modeling of High-Pressure Phase Behavior of the Carbon Dioxide + Pentan-1-ol Binary System. *J. Chem. Eng. Data* **2011**, *56*, 5000−5007.
(93) Pereira, L.; Santos, P. G.; Scheer, A. P.; Ndiaye, P. M.; Corazza, M. L. High Pressure Phase Equilibrium Measurements for Binary Systems CO_2+1-Pentanol and CO_2+1-Hexanol. *J. Supercrit. Fluids* **2014**, *88*, 38−45.
(94) Beier, A.; Kuranov, J.; Stephan, K.; Hasse, H. High-Pressure Phase Equilibria of Carbon Dioxide + 1-Hexanol at 303.15 and 313.15 K. *J. Chem. Eng. Data* **2003**, *48*, 1365−1367.
(95) Secuianu, C.; Feroiu, V.; Geană, D. Investigation of Phase Equilibria in the Ternary System Carbon dioxide+1-Heptanol+n-Pentadecane. *Fluid Phase Equilib.* **2007**, *261*, 337−342.
(96) Scheidgen, A. L. Fluidphasengleichgewichte binären und ternären Kohlendioxidmischungen mit schwerfüchtigen organischen Substanzen bis 100 MPa (Fluid phase equilibrium of binary and ternary carbon dioxide mixtures with heavy organic substances up to 100 MPa). Ph.D. Thesis, Universität Bochum: Bochum, Germany, 1997.
(97) Secuianu, C.; Feroiu, V.; Geană, D. Phase Equilibria of Carbon dioxide+1-Nonanol System at High Pressures. *J. Supercrit. Fluids* **2010**, *55*, 653−661.
(98) Fourie, F. C. v. N.; Schwarz, C. E.; Knoetze, J. H. Phase Equilibria of Alcohols in Supercritical Fluids. *J. Supercrit. Fluids* **2008**, *47*, 161−167.
(99) Jou, F.-Y.; Deshmukh, R. D.; Otto, F. D.; Mather, A. E. Vapor-Liquid Equilibria of H_2S and CO_2 and Ethylene Glycol at Elevated Pressures. *Chem. Eng. Commun.* **1990**, *87* (1), 223−231.
(100) Silva-Oliver, G.; Galicia-Luna, L. A.; Sandler, S. I. Vapor−liquid Equilibria and Critical Points for the Carbon Dioxide + 1-Pentanol and Carbon Dioxide + 2-Pentanol Systems at Temperatures from 332 to 432 K. *Fluid Phase Equilib.* **2002**, *200*, 161−172.
(101) Staby, A.; Mollerup, J. M. Measurement of Mutual Solubilities of 1-Pentanol and Supercritical Carbon Dioxide. *J. Supercrit. Fluids* **1993**, *6*, 15−19.
(102) Elizalde-Solis, O.; Galicia-Luna, L. A.; Sandler, S. I.; Sampayo-Hernández, J. G. Vapor−liquid Equilibria and Critical Points of the CO_2 + 1-Hexanol and CO_2 + 1-Heptanol Systems. *Fluid Phase Equilib.* **2003**, *210*, 215−227.
(103) Lee, M.-J.; Chen, J.-T. Vapor-Liquid Equilibrium for Carbon Dioxide/alcohol Systems. *Fluid Phase Equilib.* **1994**, *92*, 215−231.

DOI: 10.1021/acs.jced.7b00663
J. Chem. Eng. Data XXXX, XXX, XXX−XXX

(104) Weng, W.-L.; Chen, J.-T.; Lee, M.-J. High-Pressure Vapor-Liquid Equilibria for Mixtures Containing a Supercritical Fluid. *Ind. Eng. Chem. Res.* **1994**, *33*, 1955−1961.
(105) Feng, L.; Cheng, K.; Tang, M.; Chen, Y. Vapor−liquid Equilibria of Carbon Dioxide with Ethyl Benzoate, Diethyl Succinate and Isoamyl Acetate Binary Mixtures at Elevated Pressures. *J. Supercrit. Fluids* **2001**, *21*, 111−121.
(106) Weng, W. L.; Lee, M.-J. Phase Equilibrium Measurements for the Binary Mixtures of 1-Octanol plus CO_2, C_2H_6 and C_2H_4. *Fluid Phase Equilib.* **1992**, *73*, 117−127.
(107) Chiu, H.-Y.; Jung, R.-F.; Lee, M.-J.; Lin, H.-M. Vapor−liquid Phase Equilibrium Behavior of Mixtures Containing Supercritical Carbon Dioxide near Critical Region. *J. Supercrit. Fluids* **2008**, *44*, 273−278.
(108) Spee, M.; Schneider, G. M. Fluid Phase Equilibrium Studies on Binary and Ternary Mixtures of Carbon Dioxide with Hexadecane, 1-Dodecanol, 1,8-Octanediol and Dotriacontane at 393.2 K and at Pressures up to 100 MPa. *Fluid Phase Equilib.* **1991**, *65*, 263−274.
(109) Pöhler, H.; Scheidgen, A. L.; Schneider, G. M. Fluid Phase Equilibria of Binary and Ternary Mixtures of Supercritical Carbon Dioxide with a 1-Alkanol and an *n*-Alkane up to 100 MPa and 393 K—cosolvency Effect and Miscibility Windows (Part II). *Fluid Phase Equilib.* **1996**, *115* (1−2), 165−177.
(110) Kordikowski, A.; Schneider, G. M. Fluid Phase Equilibria of Binary and Ternary Mixtures of Supercritical Carbon Dioxide with Low-Volatility Organic Subtances up to 100 MPa and 393 K: Cosolvency Effects and Miscibility Windows. *Fluid Phase Equilib.* **1993**, *90*, 149−162.
(111) Hölscher, I. F.; Spee, M.; Schneider, G. M. Fluid-Phase Equilibria of Binary and Ternary Mixtures of CO_2 with Hexadecane, 1-Dodecanol, 1-Hexadecanol and 2-Ethoxy-Ethanol at 333.2 and 393.2 K and at Pressures up to 33 MPa. *Fluid Phase Equilib.* **1989**, *49*, 103−113.
(112) Artal, M.; Pauchon, V.; Embid, J. M.; Jose, J. Solubilities of 1-Nonanol, 1-Undecanol, 1-Tridecanol, and 1-Pentadecanol in Supercritical Carbon Dioxide at T = 323.15 K. *J. Chem. Eng. Data* **1998**, *43*, 983−985.
(113) Jan, D.-S.; Mai, C.-H.; Tsai, F.-N. Solubility of Carbon Dioxide in 1-Tetradecanol, 1-Hexadecanol, and 1-Octadecanol. *J. Chem. Eng. Data* **1994**, *39*, 384−387.
(114) Lam, D. H.; Jangkamolkulchai, A.; Luks, K. D. Liquid-Liquid-Vapor Phase Equilibrium Behavior of Certain Binary Carbon Dioxide + *n*-Alkanol Mixtures. *Fluid Phase Equilib.* **1990**, *60*, 131−141.
(115) Ke, J.; Reid, K. E.; Poliakoff, M. The Application of a Shear Mode Piezoelectric Sensor to Monitoring the High-Pressure Phase Behaviour of Asymmetric Binary Systems. *J. Supercrit. Fluids* **2007**, *40*, 27−39.
(116) Yeo, S.-D.; Park, S.-J.; Kim, J.-W.; Kim, J.-C. Critical Properties of Carbon Dioxide + Methanol, + Ethanol, + 1-Propanol, and + 1-Butanol. *J. Chem. Eng. Data* **2000**, *45*, 932−935.
(117) Gil, L.; Blanco, S. T.; Rivas, C.; Laga, E.; Fernández, J.; Artal, M.; Velasco, I. Experimental Determination of the Critical Loci for {*n*-C_6H_{14} or CO_2+alkan-1-ol} Mixtures. Evaluation of Their Critical and Subcritical Behavior Using PC-SAFT EoS. *J. Supercrit. Fluids* **2012**, *71*, 26−44.
(118) Byun, H.-S.; Kwak, C. High Pressure Phase Behavior for Carbon Dioxide-1-Butanol and Carbon Dioxide-1-Octanol Systems. *Korean J. Chem. Eng.* **2002**, *19*, 1007−1013.
(119) Christensen, J. J.; Cordray, D. R.; Oscarson, J. L.; Izatt, R. M. The Excess Enthalpies of Four (Carbon Dioxide + an Alkanol) Mixtures from 308.15 to 573.15 K at 7.50 to 12.50 MPa. *J. Chem. Thermodyn.* **1988**, *20*, 867−865.
(120) Scilipoti, J. A.; Cismondi Duarte, M.; Brignole, E. A. Prediction of Physical Properties for Molecular Design of Solvents. *Fluid Phase Equilib.* **2014**, *362*, 74−80.
(121) Brannock, K. C. Preparation of Sunstituted 4-Pentenals. *J. Am. Chem. Soc.* **1959**, *81*, 3379−3383.
(122) Fuller, A. E.; Hickinbottom, W. J. 589. The Synthesis and Reactions of Branched-Chain Hydrocarbons. Part XVIII. Chlorination of 2,2,4-Trimethylpentane. *J. Chem. Soc.* **1965**, 3235.
(123) Gasson, E. J.; Graham, A. R.; Millidge, A. F.; Robson, I. K. M.; Webster, W.; Wild, A. M.; Young, D. P. Oxidation Products of Diisobutylene. Part II. The Isomerisation of 1:2-Epoxy-2:4: 4-Trimethylpentanal. *J. Chem. Soc.* **1954**, 2170.
(124) Kallina, D.; Kuffner, F. Trennung Isomerer Alkohole Mittels Der Gas-Flüssig-Chromatographie, 2. Mitt. *Monatsh. Chem.* **1960**, *91*, 289−293.
(125) Quilico, A.; Grünanger, P.; Piozzi, F. Synthesis of Tetrahydro- and Perhydro-Dendrolasin. *Tetrahedron* **1957**, *1*, 186−194.
(126) Sax, K.; Stross, F. Notes - Synthesis of Squalane. *J. Org. Chem.* **1957**, *22*, 1251−1252.
(127) Inouye, H. Über Die Bestandteile von Pirola Japonica Sieb. III. *Yakugaku Zasshi* **1952**, *72*, 731−734.
(128) Sima, S.; Secuianu, C.; Feroiu, V.; Geană, D. New High-Pressures Vapor-Liquid Equilibrium Data for the Carbon Dioxide + 2-Methyl-1-Propanol (Isobutanol) Binary System. *Cent. Eur. J. Chem.* **2014**, *12*, 953−961.
(129) Inomata, H.; Kondo, A.; Kakehashi, H. Vapor−liquid Equilibria for CO_2−fermentation Alcohol Mixtures. *Fluid Phase Equilib.* **2005**, *228−229*, 335−343.
(130) Lee, H.-S.; Yong Mun, S.; Lee, H. High-Pressure Phase Equilibria for the Carbon dioxide−2-Methyl-1-butanol, Carbon dioxide−2-Methyl-2-butanol, Carbon dioxide−2-Methyl-1-butanol−Water, and Carbon dioxide−2-Methyl-2-butanol−Water Systems. *Fluid Phase Equilib.* **1999**, *157*, 81−91.
(131) Lee, H.-S.; Mun, S. Y.; Lee, H. High-Pressure Phase Equilibria of Binary and Ternary Mixtures Containing the Methyl-Substituted Butanols. *Fluid Phase Equilib.* **2000**, *167*, 131−144.
(132) Lopes, J. A.; Chouchi, D.; Nunes da Ponte, M. High-Pressure Phase Equilibrium of CO_2 + 2-Phenylethanol and CO_2 + 3-Methyl-1-butanol. *J. Chem. Eng. Data* **2003**, *48*, 847−850.
(133) Vázquez da Silva, M.; Barbosa, D. High Pressure Vapor−liquid Equilibrium Data for the Systems Carbon dioxide/2-Methyl-1-Propanol and Carbon dioxide/3-Methyl-1-butanol at 288.2, 303.2 and 313.2 K. *Fluid Phase Equilib.* **2002**, *198*, 229−237.
(134) Kodama, D.; Kato, M.; Kaneko, T. Volumetric Behavior of Carbon dioxide+2-Methyl-1-propanol and Carbon dioxide+2-Methyl-2-propanol Mixtures at 313.15 K. *Fluid Phase Equilib.* **2013**, *357*, 57−63.
(135) Găinar, I.; Bala, D. The Solubility of CO_2 in Some C4 Alcohols at High Pressures. *Analele Univ. din Bucuresti* **2004**, *I−II*, 213−273.
(136) Chen, H.-I.; Chen, P.-H.; Chang, H.-Y. High-Pressure Vapor - Liquid Equilibria for CO_2 + 2-Butanol, CO_2 + Isobutanol, and CO_2 + Tert-butanol Systems. *J. Chem. Eng. Data* **2003**, *48*, 1407−1412.
(137) Wang, L.; Hao, X.; Zheng, L.; Chen, K. Phase Equilibrium of Isobutanol in Supercritical CO_2. *Chin. J. Chem. Eng.* **2009**, *17*, 642−647.
(138) Gros, H. P.; Bottini, S. B.; Brignole, E. A. A Group Contribution Equation of State for Associating Mixtures. *Fluid Phase Equilib.* **1996**, *116*, 537−544.
(139) Mansoori, G. A.; Carnahan, N. F.; Starling, K. E.; Leland, T. W., Jr. Equilibrium Thermodynamic Properties of the Mixture of Hard Spheres. *J. Chem. Phys.* **1971**, *54*, 1523−1525.
(140) Fredenslund, Å.; Gmehling, J.; Rasmussen, P. *Vapor−Liquid Equilibria Using UNIFAC. A Group Contribution Method*; Renon, H., Ed.; Elsevier Ltd: Amsterdam, 1977; Vol. *1*, pp 27−64.
(141) Abrams, D. S.; Prausnitz, J. M. Statistical Thermodynamics of Liquid Mixtures: A New Expression for the Excess Gibbs Energy of Partly or Completely Miscible Systems. *AIChE J.* **1975**, *21*, 116−128.

DOI: 10.1021/acs.jced.7b00663
J. Chem. Eng. Data XXXX, XXX, XXX−XXX